Paper 045-II

ACTIVE ROTOR CONTROL FOR HELICOPTERS: INDIVIDUAL BLADE CONTROL AND SWASHPLATELESS ROTOR DESIGNS

Ch. Kessler
DLR, Institute of Flight Systems, Lilienthalplatz 7, 38108 Braunschweig, Germany

Abstract

Modern helicopters still suffer from many problems that hinder a further increase in their efficiency, acceptance and hence their market share. The high level of vibrations and the noise generated by the rotor are the most important reasons for this. Vibrations are problematic for pilot and passenger comfort, but give also rise to an increase in maintenance effort. The high noise level limits the acceptance of helicopters in the public, e.g. landing of helicopters on or close to hospitals during Emergency Medical Services missions. High noise levels also lead to an early aural detection during military missions. Further drawbacks of helicopters are the high fuel consumption in high-speed forward flight and hence low range, limited speed of flight, etc. To overcome these drawbacks active rotor control technologies have been investigated for a long time. Many different approaches have been investigated and most of them are not being followed any more. First investigations started with so-called Higher Harmonic Control (HHC) which has been replaced by Individual Blade Control (IBC). In a previous paper motivation on active rotor control technology was recapitulated as well as achievements on HHC. This paper continues that work and gives a survey on IBC concepts and achievements. An outlook on the idea of the swashplateless helicopter concludes the paper.

1. INTRODUCTION

In 2007, the helicopter community celebrated 100 years of helicopter flight. Since the early developments, helicopters experienced tremendous improvements in performance, safety, controllability and handling qualities. Helicopters conquered their market and can not be replaced by any other aircraft. The ability to take off and land vertically and to hover as well as the excellent low-speed flight performances and handling qualities in comparison to other VTOL aircraft enables and consolidates this success. On the other hand, helicopters still suffer from many problems that hinder a further increase in their market share. The first drawback is the high vibration level when compared to fixed-wing airplanes. Although a tremendous reduction in vibration levels has been achieved, from 0.3 – 0.5g mid of the 1950s down to 0.1g or even somewhat below mid of the 1990s by passive absorbers and proper dynamical design, this trend runs into saturation and especially the ambitious level recommended by a NASA council of 0.02g , see [1], does not seem to be within reach. Some helicopters now use actively controlled absorbers in the cabin. Origin of the vibrations is the inhomogeneous flow seen by the rotor blades during rotor revolution. All fuselage mounted absorbers do not fight the vibrations at their source. Some absorbers try to counteract vibrations already in the rotating frame, but they as well do not reduce the flow inhomogenity. While vibrations are problematic for pilot and passenger comfort, they give also rise to an increase in maintenance effort and costs. In addition, the high noise levels limit the acceptance of helicopters in the public, e.g., landing of helicopters on or close to hospitals during Emergency Medical Services missions. This is the second drawback of helicopters. Especially the noise generated during descent is annoying, since the helicopter comes closer to the ground. This noise is known as blade vortex interaction (BVI) noise. Other noise sources are related to blade loading, the thick airfoil pushing away the air while moving, high Mach numbers at the advancing blade, etc. High noise levels also lead to an early aural detection during military missions. As for the vibrations, passive measures (i.e. proper blade design) can reduce the noise level by several dB when compared to older blade designs like rectangular blades with constant airfoil distribution. Further drawbacks of helicopters are the high fuel consumption in high-speed forward flight, the limited speed of flight, the low transport capacity, the low range, etc.

This situation motivated world wide research on and development of active rotor control technology. First research on active rotor control started in the early 1950s addressing the principle of Higher Harmonic Control (HHC) to alleviate typical helicopter problems. Although these theoretical studies tried to alleviate blade stall through HHC, the main focus shifted later to vibration and noise reduction. Much theoretical work and many test campaigns investigated the benefits of HHC and tried to explore how HHC alters the flow field around the rotor. Even some flight test demonstrators were built to prove HHC benefits in a real helicopter environment. Refs. [1] and [2] give a survey on HHC results, the latter the status till 1995 and with special focus on vibration reduction. HHC is based on actuators located below the swashplate, thus limiting mechanically the applicable control frequencies in the rotating frame for rotors with more than three blades. This implies for a helicopter with four blades a limitation to the following frequencies:

3, *4*, *5/rev* and integer multiples of *4/rev* plus the next harmonics before and after it (e.g. *7*, *8*, *9/rev* …). The very useful *2/rev* frequency cannot be controlled. This is a severe drawback. Nevertheless, HHC has demonstrated to reduce noise by up to 5-6dB and vibrations by up to 90%, however, not simultaneously or at least not simultaneously in a sufficient manner. In addition, the reduction of power consumed and stall delay require *2/rev* control. Both problems led researchers to finally conclude that Individual Blade Control (IBC) is highly desirable. Therefore, the focus on active rotor control was shifted towards IBC although HHC has advantages in terms of system simplicity.

IBC is based on actuators in the rotating frame and thus overcomes the limits inherent to HHC. Research on IBC started in the 1980s. Active control concepts featuring actuators in the rotating frame were also used in the 1960s, but were not called IBC. Many IBC concepts have been designed and tested, both in wind tunnel as well as in flight. Early concepts focussed on blade root actuation. Hydraulic actuators replaced the control rods that connect the swashplate with the pitch horns. Advanced designs address the principle of smart actuation driving a trailing edge flap. Even more advanced applications of smart actuation integrate distributed actuators into the blade (blade spar or skin) to generate active twist along the rotor span. Further concepts are nose droop or leading edge flaps, Gurney flaps or soft trailing edges, multi-swashplate systems and so on. Despite more than 50 years of R&D on rotor active control, no serial production helicopter makes use of such a system. This fact is attributed to the challenging requirements like minimum system complexity, high reliability and effectiveness, minimum weight, costs and last but not least the high loads acting on the blades.

2. SURVEY ON INDIVIDUAL BLADE CONTROL

The definition of IBC varies in the literature. Sometimes, IBC is defined as a system that is fully integrated in the rotating frame with individual hardware (sensors, actuation, etc.) for each blade. This definition has been introduced by HAM [15] to [20]. HAM and his team at MIT have demonstrated in many applications how well his concept works. From time to time, IBC is understood just as a blade root actuation system. This wording tries to distinguish blade root actuation from other concepts such as active flap or active twist actuation. This survey defines IBC as a system featuring as many control degrees-of-freedom as the rotor has blades no matter which type of actuation is used and no matter where sensors, power supply etc. are integrated. In this respect, this definition is a direct extension of the one given in [1] (there, it has been distinguished from HHC by having actuators in the rotating frame). The reason for this extended definition will be explained in section 2.4.

Many different actuation concepts have been studied and some of them have been tested in wind tunnel and flight. Commonly used actuation concepts are shown in Figure 1. The blade root actuation concepts make use of hydraulic actuators that replace the push rods between the upper rotating swashplate and the blade pitch horn. The other two designs make use of smart actuation technology by integrating either local or distributed piezo-ceramics into the blade. The smart flap concept needs sophisticated amplification of the very small piezo-stack stroke. Friction at hinges and elasticity of the leverage system are problematic. The active twist concept is free of any mechanical amplification or moving parts. A comprehensive survey on smart structures technology and smart actuation is given by CHOPRA [3]. The paper also describes alternatives to piezo-ceramic stack actuation like shape memory and magnetostrictive alloys or piezo-ceramic bimorph actuation. Today, piezo-ceramic stack actuators driving a trailing edge flap make use of different amplification concepts. The first uses a steel frame for strain amplification. To save weight, fibre composite material is currently investigated to replace the metal frame. Alternatives are L-arm, double L-L amplification [3] or the X-frame actuator, see section 2.2. Recently, large stroke actuators have been presented to drive a trailing edge flap [84], [85]. The first is an electromechanical actuator (EMA), the other a pneumatic artificial muscle (PMA). Since both concepts address IBC, but also primary control, more explanations on both actuators can be found in section 3.

Figure 1: Actuation concepts for IBC.

Further active rotor control concepts are listed in Figure 2. The first is a movable Gurney or micro flap. The Gurney flap is a small tab typically less than 5% of airfoil chord in height and is attached normal to the airfoil centreline. Fixed flaps were used by Dan Gurney on race cars to increase the downward force generated by the spoiler. A numerical comparison of Gurney flaps with trailing edge flaps is given in [4]. The other concepts are active trailing edge tabs, leading edge flap and active trailing edge. Active tabs were investigated in two variants. One performs a straight motion (a), the other small angular deflections (b). Concept a) was studied in [5], [6] and [7]. Ref. [5] studied a translatory extendable tab that deploys up to 30% of the blade chord. It uses the effect of variable blade area. In [6] and [7], a fixed tab bend angle was added. Ref. [7] used 10° tab bend angle. Maximum extension was 10% of the blade chord. However, its “value of technology” was rated in [8] as poor. Concept b) is taken from [9]. This concept is covered by the trailing edge flap concept in Figure 1. Active leading edge flaps were investigated in context with dynamic stall alleviation. 2D wind tunnel testing and theoretical investigations revealed benefits of this concept [10], [11]. Design of leading edge flaps was deemed to be rather complex by some helicopter manufacturers. Actuator forces are quite high due to the large pressure difference between upper and lower airfoil surface. The structural integrity of the blades is even more difficult, since this flap harms the spar at the leading edge and blade design becomes problematic. The active trailing edge uses the concept of morphing cross sections and it aims to twist the blade using the servo effect. It can be interpreted as a structurally integrated flap. Piezo-based bending actuators were proposed in [12]. The deflecting ends of the actuators are embedded in flexible filler to retain a smooth contour of the airfoil. A further variant is the active pitching tip [13], [14]. It may be viewed as a flap with a flap chord to airfoil chord ratio of one. A recently emerged concept is the use of a multi-swashplate [80].

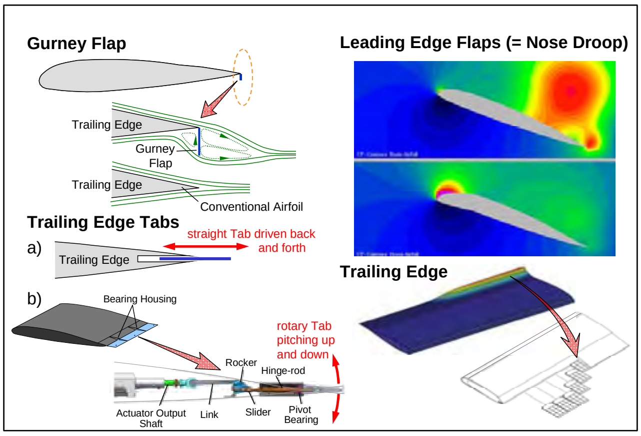

Figure 2: Further concepts for active rotor control.

This paper reviews the results gathered so far with the actuation concepts of Figure 1. They are the most widespread ones. In addition, the principle of the multi-swashplate will be outlined, since it has never been investigated before.

2.1. Blade Root Actuation

As the deficiency of HHC became evident, attention was directed towards IBC. First work on IBC was done by KRETZ, see chapter 2.2. Inspired by this work, HAM started at MIT to investigate and promote the idea of IBC. His name is associated with IBC as hardly any other. Overviews on the IBC research at MIT are given in [15] and [16]. According to his definition, IBC is capable of controlling each blade independently from each other and features one feedback loop per blade in the rotating frame by using blade-mounted sensors. He showed that IBC using a swashplate is feasible, too [17]. Figure 3 shows the frequency band required by IBC. It comprises a low-frequency (LF) domain ranging from *0* to *1/rev* involving helicopter gust response, flying qualities, blade instabilities and ground resonance. The high frequency (HF) domain covers frequencies above *1/rev* for blade bending stress, vibration and stall flutter [18]. Pilot control occurs at *1/rev* and it is essential that IBC does not degrade cyclic control effectiveness.

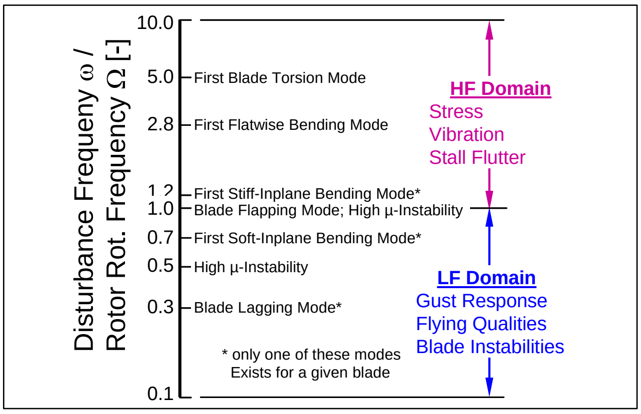

Figure 3: IBC frequency domain according to HAM.

HAM has demonstrated a broad variety of applications using simple models to tune feedback gains and tested his concepts on small wind tunnel models. Applications covered gust and stall alleviation, attitude stabilisation, blade lag damping augmentation, stall flutter suppression, blade flapping stabilisation, vibration reduction and performance enhancement. He pointed out: it would be most effective if the IBC system would comprise several sub-systems, each controlling a specific mode such as flapping, lagging or torsion. Each sub-system then would operate in its appropriate frequency band. Undesired frequency content in the measured sensor signals would be eliminated by filtering. In various applications he used blade-mounted accelerometers to get the measurements for the feedback loop. This idea of modal decomposition is outlined in [18], [19].

In contrast to the T-matrix approach to control vibrations, see [1], HAM used feedback accelerometer signals from three different blade stations. Flapping acceleration was fed back in the inner loop and blade flatwise bending rate (integrated from first flatwise bending acceleration) in the outer loop. Simple proportional feedback gains were used to close the loop. The success of this simple approach is shown in Figure 4. Bending response was reduced by 75% in an experiment.

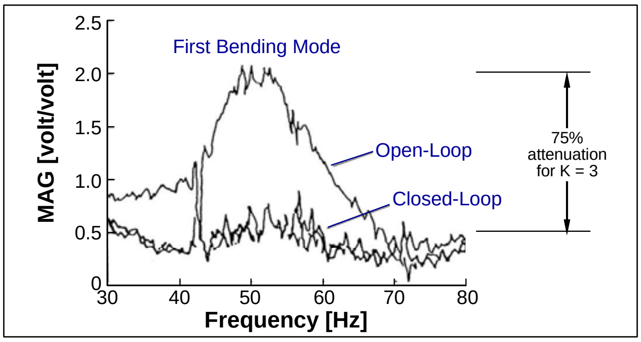

Figure 4: Open- and closed-loop tip accelerometer response to white noise pitch input in hover.

Gust alleviation was demonstrated in [19]. The paper presents wind tunnel experiments at various advance ratios which show a substantial alleviation of the blade flapping response to gusts. Lead-lag damping augmentation is shown in [20]. This paper, too, compares results gathered with a simple mathematical model to wind tunnel experiments. Lag rate (integrated from two accelerometer signals) was fed back to blade pitch. The mathematical equations were based on an isolated blade undergoing lag and flap motion. No aerodynamic excitation of the lag motion was considered. The mechanism to control lead-lag was the excitation of flapping and the resulting lead-lag motion through Coriolis coupling. Inflow was neglected. This approach is rather simple. A compensator was included in the feedback loop. Simple proportional feedback (gain K_R) was used to close the loop. The result is shown in Figure 5. Using these relations, lead-lag damping has been increased.

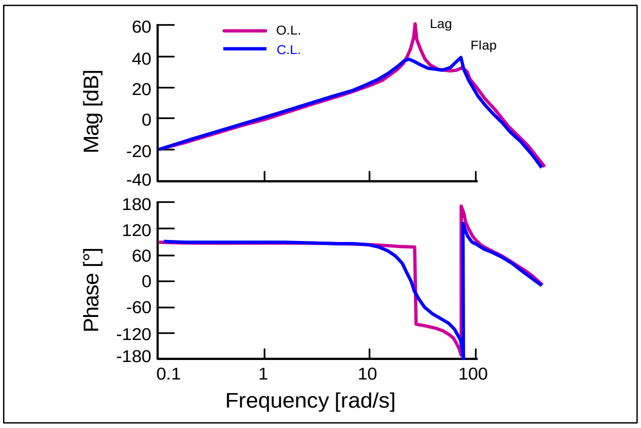

Figure 5: Open- and closed-loop ($K_R = 4$) Bode plot from voltage pitch input to lead-lag angle for wind tunnel model.

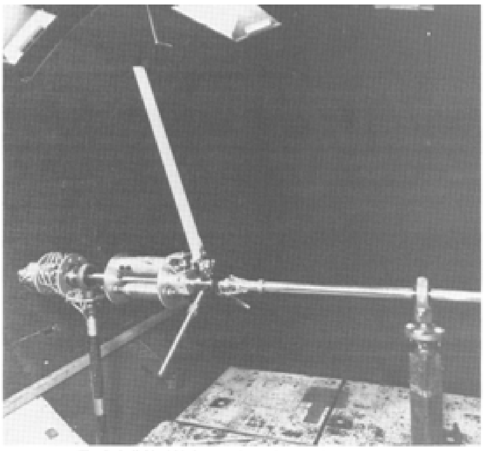

Figure 6: IBC experimental rig at MIT.

The wind tunnel model is shown in Figure 6. Comparison between theory and experiments revealed some discrepancies. The predicted lag acceleration response was higher than the measured one. Looking at the Bode plots for the wind tunnel model, no lag-damping augmentation from the amplitude diagram was visible. Nevertheless, the phase diagram showed a slight reduction in phase slope at lag resonance frequency on closing the loop.

The idea of lag damping augmentation by IBC was picked up in [21] and compared to lead-lag stabilisation via swashplate control. The model considered body dynamics and fully coupled flap-lag motion. Two-dimensional blade element theory was used to compute aerodynamic blade loads. Inflow was constant over the rotor disc. Model data were similar to a Bo 105. Fuselage damping was reduced to destabilize ground resonance. The paper showed that both, Coriolis and aerodynamic forces, contribute to lead-lag control. For stabilising the unstable body pitch lead-lag mode proportional feedback of the lag angle, lag rate and lag acceleration was chosen. The study revealed that it was not sufficient to optimise feedback gains on an isolated rotor blade. The isolated rotor blade (no body dynamics) showed 0.029 damping ratio without feedback compared to 0.08 in the closed-loop case applying appropriate gains. When applied to the coupled rotor/body model, the feedback gains optimised on the isolated rotor blade even increased the pitch lag instability. The same happened for feedback gains optimised for the coupled rotor/body system: the instability was stabilised although stability was poor, but the isolated blade was even destabilised by closing the loop. Classical feedback of body pitch attitude, pitch rate and pitch acceleration could stabilise ground resonance quite successfully and turned out to be superior to the IBC approach [21].

The idea of increasing lead-lag damping through IBC was also investigated in [22]. The numerical study considered an isolated rotor, however, rigid blade dynamics (flap, lag and torsion) were considered, as well as a quasi-steady application of Greenberg's theory. Inflow was computed from Drees' model. Moderate open-loop lead-lag damping occurred at moderate advance ratios. Feedback of lead-lag states increased lag damping from hover to an advance ratio of μ = 0.4 even for fixed gains optimised for hover. Gain scheduling with advance ratio maximised lead-lag damping on the expense of large blade pitch amplitudes.

The idea of stall flutter suppression was investigated in [23]. Stall flutter is a phenomenon that may occur at high advance ratios or high blade loading. Stall flutter is problematic over only a small part of the rotor azimuth. The excitation damps out when the rotor blade swings around to the advancing side. Even though the rotor blade may then be stable again, this leads to an increase in control system loads. A stall flutter suppression system would be a system that would eliminate pitch excitation on the retreating side. Figure 7 (top) shows such an idealised stall flutter suppression system. Pitch rate was fed back to the actuator input to increase pitch damping. Pitch rate was derived from integrating pitch acceleration measured by two blade-mounted accelerometers. The arrangement of the accelerometers aimed at eliminating the influence of the propeller moment, while some flapping and cyclic effects could not be eliminated. The wind tunnel model was similar to the one shown in Figure 6. This simple system has been tested in the wind tunnel, first non-rotating, than rotating at advance ratios of about 0.3 and finally at 0.33. The latter case caused severe stall flutter excitation. Experimental results at μ = 0.3, both open- and closed-loop using simple proportional feedback of pitch rate, are shown in Figure 7 (bottom) for pitch acceleration time history and Fast Fourier Transformation (FFT) of pitch acceleration. The time histories show the *1/rev* cyclic input superposed by small pitch oscillations caused by stall as the high frequency peaks. On closing the loop, the high frequency peaks became smaller. This can be seen clearly in the FFT. The green line denotes the cyclic trim. The other peaks in the FFT are stall-induced high-frequency pitching motions. The closed-loop FFT shows smaller high-frequency peaks than the open-loop case illustrating the success of this idea. The difference in the offset of the pitch acceleration time history was caused by different calibration.

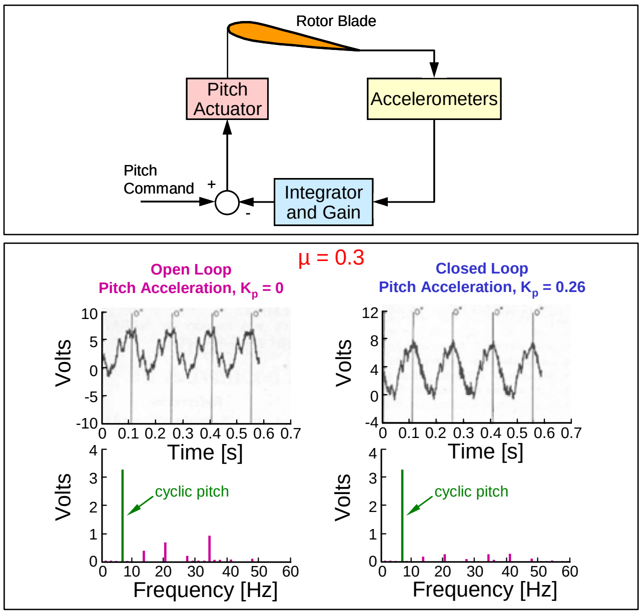

Figure 7: Idealised stall flutter suppression system (top) and open- and closed-loop responses (bottom) of pitch acceleration, time histories and FFT, μ = 0.3, K_p = gain.

A numerical analysis of open- and closed-loop stall alleviation and performance improvement was conducted in [24]. The model was based on an improved UMARC computer code, see [24] for details. Basis helicopter was a UH-60 at μ = 0.236 and high blade loading C_T/σ = 0.13. Open- and closed-loop IBC using *2/rev* to *6/rev* harmonics was investigated. Open-loop investigations revealed that *2/rev* could reduce stall moderately. The optimum amplitude turned out to be 1°, the optimum phase 210°. The other harmonics were less effective. Minimisation of shaft torque (power) using *2/rev* IBC was found to be best at 60° phase using 1° amplitude. No amplitude sweep was performed. The relations were mentioned to be highly non-linear. The closed-loop approach was based on a linear T-matrix formulation and was in general not successful. Probably, the highly dynamic and non-linear blade stall phenomenon may not be captured well enough using linear T-matrix formulations.

Wind tunnel testing of a full-scale Bo 105 rotor with servo-hydraulic IBC was performed in the 40x80ft² wind tunnel at NASA Ames in 1993 and 1994 [25], [26][1]. The rotor test apparatus (RTA) and the IBC system are shown in Figure 8. The objectives were vibration and BVI noise reduction as well as performance improvement. This was the first full-scale wind tunnel test to explore these issues.

Figure 8: Bo 105 rotor and RTA in wind tunnel and close-up view on the IBC system.

[1] Partners were NASA, US Army, ZF Luftfahrttechnik (ZFL), DLR and Eurocopter Germany.

During the 1993 campaign a minimum flap trim method was used, rotor hub moments were not re-trimmed with each IBC input during these tests. In 1994, thrust and rotor moments were re-trimmed, but not propulsive force. Therefore, performance related conclusions have to be considered carefully. IBC inputs covered *2/rev* to *6/rev* inputs. Single and multi-harmonic combinations were applied as well as pulses, wavelets and doublets approximated by combining various harmonics. The actuators were limited to ±3° blade pitch variation. This maximum amplitude reduced down to about ±1.5° at *6/rev*. Test conditions covered advance ratios from μ = 0.1 to 0.45. Figure 9 shows the change in *4/rev* hub loads for a phase sweep at constant amplitude as well as for an amplitude sweep at optimal phase at 43kts (μ = 0.1) by *2/rev* IBC.

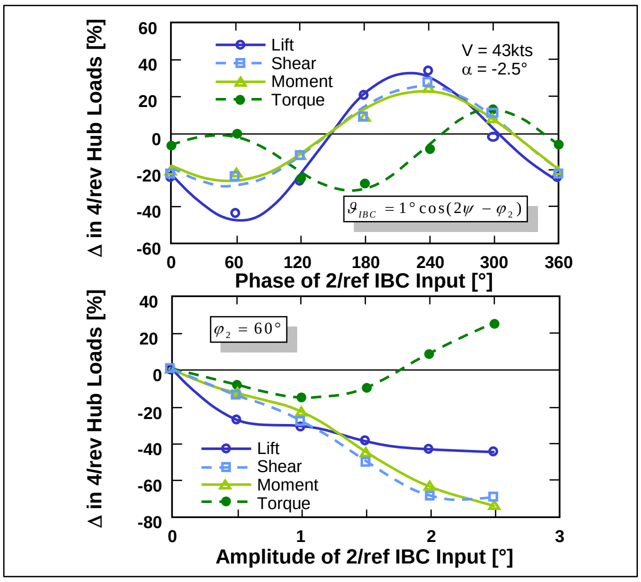

Figure 9: Impact of *2/rev* IBC on hub vibrations, 43kts (μ = 0.1), C_T/σ = 0.078, shaft angle α_S = -2.5°.

This has not been demonstrated for a 4-bladed rotor before. The values for ‘moment’ and ‘shear’ were computed from rolling and pitching moments and side and drag forces, respectively. The significant impact of *2/rev* IBC on the *4/rev* vibrations becomes evident. The optimal phase is about 60°. An amplitude of 2.5° leads to a vibration reduction of 70 to 75%. Similar trends were observed for *3/rev* and *4/rev*, but not for *5/rev* and *6/rev* IBC at that speed. It later turned out that the IBC amplitudes were too large for the higher IBC frequencies. IBC of *2/rev* and *3/rev* not only reduced *4/rev* vibrations, but also those at *8/rev*. Vibration reduction at 127kts (μ = 0.3) was more difficult due to a large amount of unsteadiness in the data.

One method to gain more insight into the mechanism of vibration reduction are polar plots. Sine and cosine components of the vibratory loads measured during phase sweep are plotted versus each other. A linear system generates circular or elliptical paths. One example for rolling and pitching moments is shown for *3/rev* IBC in Figure 10. The pitching moment shows an almost linear behaviour. It would be fully linear, if the amplitude variation would result in a straight line. For a single load one can directly determine the right IBC amplitude and phase. The chosen amplitude of 1° was too large in this case. The optimum amplitude would result in an ellipse through the origin symbolised by the dashed, grey curve. The linear relation between vibrations and IBC, see [1], stated below the figure represents this behaviour sufficiently. In contrast, the rolling moment shows a different behaviour. The measurements are highly non-linear and that data are hard to interpret. The non-linear relation shown below the figure (with matrices T_1 and T_2) would probably match the measurements and result in a curve showing more the form of an "8" instead of an ellipse. However, conclusions would still be difficult to draw. More information on this non-linear T-matrix formulation can be found in [32]. Additionally, six graphs for three forces and three moments result from the balance of the wind tunnel model. This further complicates the choice of the right amplitude/phase combination.

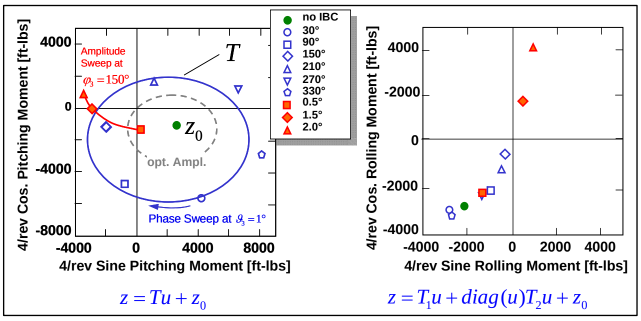

Figure 10: Impact of *3/rev* IBC on rolling and pitching moments, 43kts, $C_T/\sigma = 0.078$, shaft angle $\alpha_S = -2.5°$.

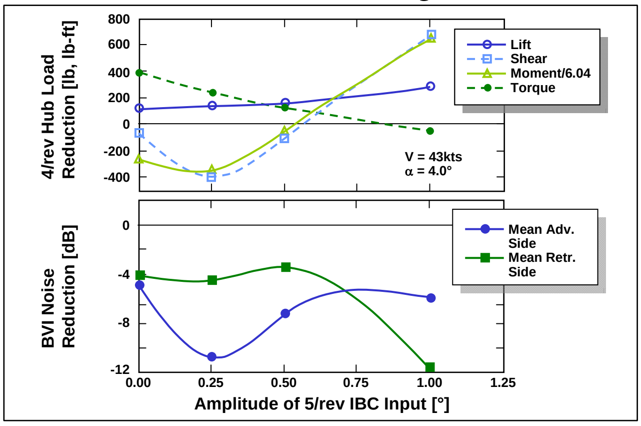

Figure 11: Simultaneous noise and vibration reduction, IBC blade pitch: $\vartheta_{IBC} = 1.5° cos(2\psi - 60°) + \vartheta_5 cos(5\psi - 210°)$, 43kts ($\mu = 0.1$), $C_T/\sigma = 0.075$, shaft angle $\alpha_S = 4°$.

During the same 1994 campaign noise measurements were done by four traversing microphones below the advancing rotor disc and three stationary ones at the retreating side. Again, *2/rev* IBC was very powerful to reduce BVI noise. Two noise minima at 60° (see vibration results!) and between 210° and 300° were determined. Noise reductions of 6-7dB on the advancing side were reported. Relations were more complex at the retreating side. Noise reductions of 5-6dB were mentioned. The optimum phase angles were found out to be either 60° or 140°-300° depending on the test condition. Nevertheless, simultaneous noise reduction on both sides would be possible. Noise reduction on both sides was also achieved by *3/rev*, but was less effective than *2/rev* and choosing one optimum phase for all test conditions was more difficult. Simultaneous noise and vibration reduction using *2* and *5/rev* IBC at varying *5/rev* amplitude (ϑ_5) can be seen in Figure 11. While torque and lift are above baseline level all other values are well below for *5/rev* amplitudes smaller than 0.5°.

Performance was improved by 7% using *2/rev* in high-speed forward flight. Considering hydraulic power requirements, a net power benefit of 3% was mentioned. Since propulsive force varied between -5 and +7.2%, ref. [27] suggests to address the lift-to-drag ratio $L/D = C_L/(C_D + C_P/\mu)$, C_P = power coefficient, instead of power. A *2/rev* phase sweep at 1° amplitude increased the reference value of 6.3 by 8.6% at 230° phase. The optimum phase for power reduction was 180°. Ref. [27] also suggests a morphological scheme to select appropriate frequencies for noise, vibrations, performance, blade load and pitch link load reduction. Following this scheme, *2/rev*, *$(N_{BL}$-1)/rev and N_{BL}/rev* are the most valuable IBC frequencies. In addition to the exploration of IBC benefits this campaign also intended to back-up a Bo 105 flight test campaign in Germany and to allow higher IBC amplitudes.

Testing of a flight-worthy IBC system started in 1990 in a joint programme between MBB and ZFL. Flight testing was conducted for 15 years on the helicopter shown in Figure 1 top left. The IBC amplitudes tested first were ±0.16° and later on ±0.42° [28], [29]. More information on the development of the IBC actuators can be found in [28]. With increasing flight test experience and confidence in the system reliability, the actuator authority has been increased to 1.1° [30]. A broad variety of papers has been published. References [28] to [34] might be representative for others. More information on the Rotor Active Control Technology (RACT)[2] project as well as on the Bo 105 test bed are summarised in [30]. The paper first shows blade pressure data without and with IBC gathered during descent. The pressure signals clearly showed the typical high frequency variations at the advancing and retreating side, caused by BVI without IBC. These peaks were reduced clearly with IBC of *2/rev*, 0.4° amplitude and 30° phase. Reference [31] gives some more insight into noise and vibration results. Figure 12 shows noise levels measured on ground during a descent. Three microphones were used. The maximum noise reduction was about 5dBA at 60° phase and 1° amplitude. This matches the wind tunnel results. Slight differences might be explained by different trim conditions and/or microphone positions. Applying *3/rev* at 0.5° amplitude was also successful in reducing noise, but less effective than *2/rev*. The optimum phase turned out to be 180°.

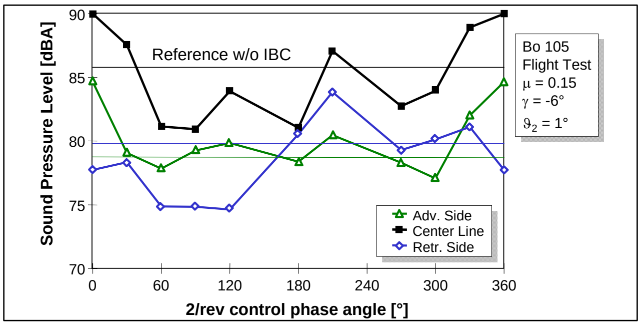

Figure 12: Noise flight test data versus phase for *2/rev* IBC, $\mu = 0.15$, descent angle $\gamma = -6°$, IBC amplitude $\vartheta_2 = 1°$.

[2] Partners were Eurocopter, ZFL, DLR and the Technical University of Braunschweig

Vibrations were measured at the co-pilot seat and at the gearbox in all three directions. Figure 13 shows *4/rev* co-pilot seat vibration for *2* and *3/rev* IBC. Excellent co-pilot seat vibration reduction was achieved at *2/rev*, 1° amplitude and 60° phase. The same was observed for the gearbox vibrations. The controlled *3/rev* amplitude of 0.5° turned out to be too large. The optimal amplitude of 0.37° was identified offline. Calculated vibrations with this amplitude were added to the figure. Vibrations were reduced by about 70% for all six measurements. These results clearly indicate the value of the *2/rev* frequency. Therefore, ref. [32] took a closer look on the importance of *2/rev* IBC and tried to explain how *2/rev* IBC manipulates *4/rev* vibrations in the fuselage. This effect was seen in inter-harmonic coupling caused by parameter excitation of periodic systems or impulsive forcing. The paper also gives a valuable survey on some HHC and IBC tests in tabular form. Equations for a non-linear T-matrix approach, see Figure 10, were also derived. This non-linear T-matrix approach matched experimental results quite well.

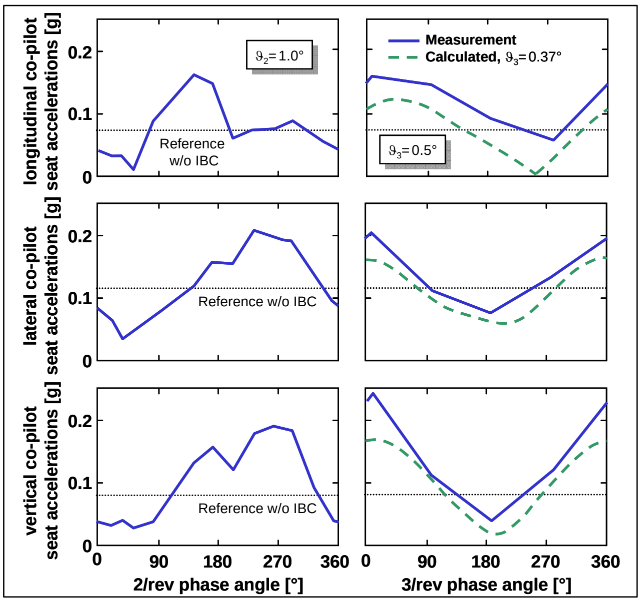

Figure 13: *4/rev* vibrations in flight at the co-pilot seat versus phase for *2* and *3/rev* IBC, μ = 0.15.

Closed-loop BVI noise reduction has been demonstrated in [33] by minimising a so-called BVI index. Preceding investigations showed that *2/rev* IBC of all IBC frequencies achieved the highest noise reduction at about 60° phase. The optimum phase was robust against small variations in descent angle. The noise reduction increased with higher IBC amplitudes. To realise closed-loop IBC control, on-board sensors are needed. It was decided to use skid-mounted microphones instead of blade-mounted sensors, e.g. pressure sensors. How well the skid microphones correlate with ground-based ones is shown in Figure 14.

The BVI index was defined as the quadratic pressure level of the typical BVI frequency range normalised by the sum of all harmonics. Figure 15 shows the applied control algorithm. The computed BVI index was time averaged over approximately four rotor revolutions to assure stability of the controller. The controller used a fixed *2/rev* IBC amplitude of 1°. Optimisation of IBC phase using a "Golden section" algorithm was restricted to 0° to 120° to guarantee fast control. The threshold algorithm was based on three controller states. If threshold "1" was exceeded (identification of BVI), the controller was activated for the first time and was switched from its "stand-by control off" modus to "search BVI minimum". The IBC phase was optimised in this state within the given range. Once a minimum was identified, the controller state changed to "BVI minimum found". The phase was kept constant unless a second threshold was exceeded. This triggered the restart of phase optimisation.

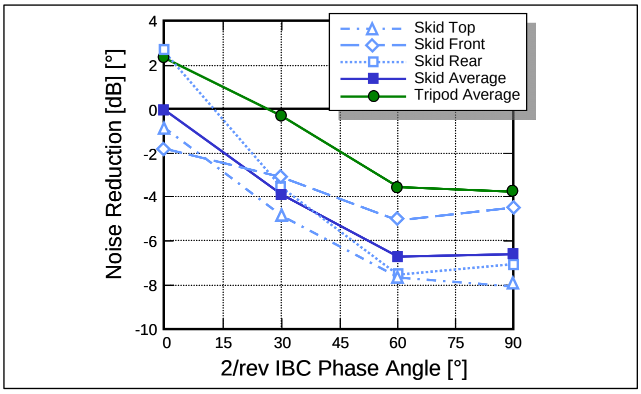

Figure 14: Comparison of skid-mounted with ground-based microphones using *2/rev* IBC.

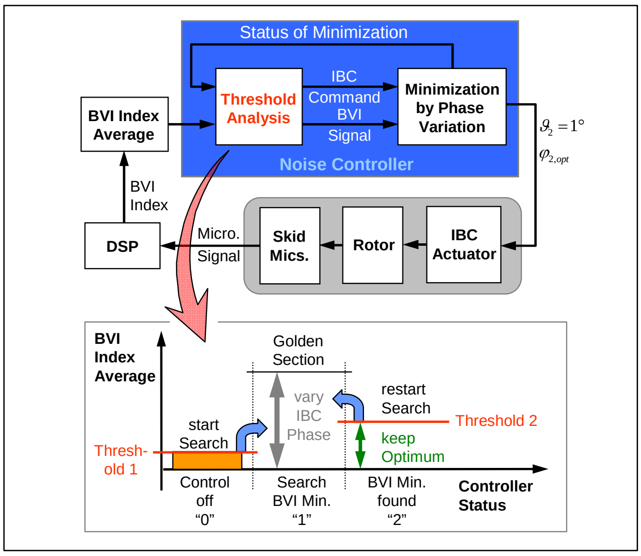

Figure 15: BVI noise control concept and logic of threshold algorithm.

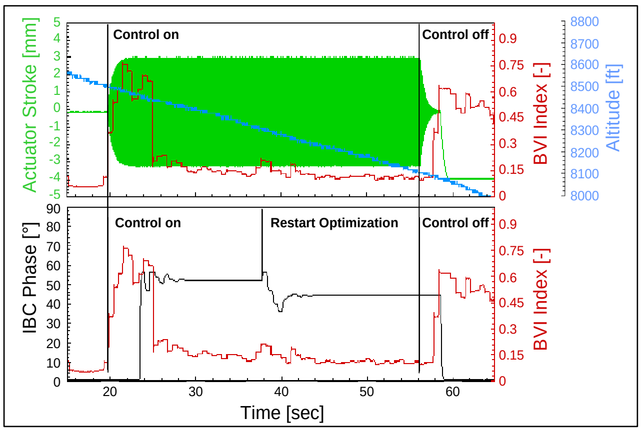

Figure 16: BVI noise reduction during descent at 600ft/min.

How well this worked is shown in Figure 16. Once the controller was activated, seen by the rising actuator stroke, the BVI index was reduced unless the control was switched off again. The success of the algorithm was verified with ground-based microphones. The reduction of the BVI index corresponded to a 5dB reduction in sound exposure level.

Finally, a closed-loop IBC campaign was conducted to explore vibration reduction by using sensor signals in the rotating frame [34]. The controller was of a disturbance rejection type. Minimisation of *4/rev* fuselage vibrations was achieved by eliminating *4/rev* hub force and moment excitations. The theoretical background and the design of the controller are outlined in [35]. In general, three forces and three moments, (F_X … M_Z) excite the fuselage. Out of these six variables, three were retained for the demonstration campaign: M_X, M_Y and F_Z. The controller approach is illustrated in Figure 17. Disturbance rejection was achieved by *4/rev* notch filters. This introduced transmission zeros into the closed-loop system thereby enforcing the elimination of the three controlled output variables at *4/rev*.

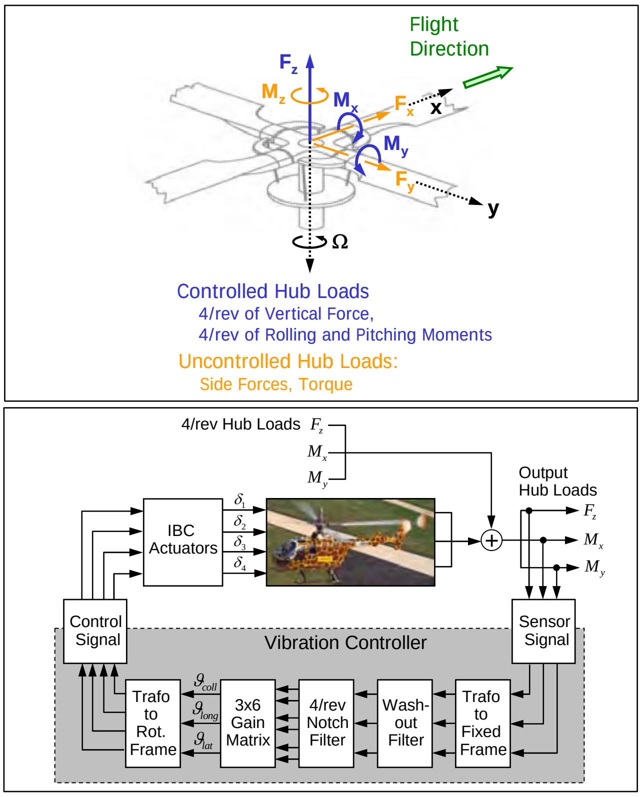

Figure 17: Hub loads for feedback control and disturbance rejection controller.

This controller approach is time domain based. Strain gauges applied to the rotor hub (for measuring flap bending moments to compute F_z) and shaft (for measurement/derivation of M_x and M_y in combination with a coordinate transformation) were used. Accelerometers at the gearbox and in the cabin were used to confirm the control approach. Flight testing covered level flight at 60 to 100kts including rotor speed variations from 98% to 102% at 100kts, climb/descent at 65kts and climb rates of ±1000ft/min and turns at 80kts and bank angles up to 30°. The presented controller approach worked very well during all flight phases. *4/rev* of F_z was reduced by 80% and M_x and M_y by 90% in level flight and 100% rpm. Variations in rpm did not reduce the controller performance. Figure 18 shows the *4/rev* vibrations in level flight plotted versus speed as one example. It shows the success of the approach. The small effect of the controller on vertical cabin vibrations was explained by neglecting the uncontrolled hub loads. Similar results were gathered for the other flight conditions.

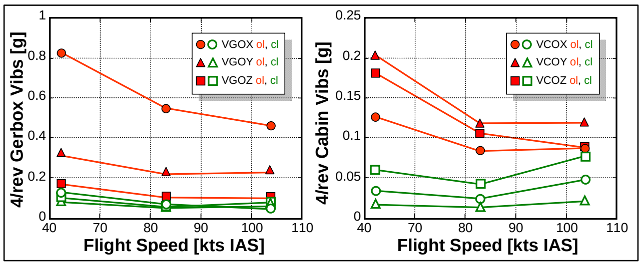

Figure 18: *4/rev* vibrations at gearbox (VGO) and cabin (VCO) in level flight versus speed, 100% rpm.

Flight testing of a blade-root IBC system on a 6-bladed CH-53G helicopter was conducted by ZFL from 2001 to 2004. The test bed is shown in Figure 1, top right. The usable actuator amplitude was about 1.1° blade pitch angle. The test campaign was conducted in an open-loop phase with maximum controlled amplitudes of 0.67° [36] and a closed-loop phase with full authority [37], [38]. Main focus of the first phase was on vibration, BVI noise, control load and rotor power reduction. The aircraft was equipped with accelerometers in the cabin at main gearbox, pilot seat, cargo compartment and tail rotor transmission, strain gauges to monitor various loads, flap and lag angle potentiometers, microphones etc. Noise reduction trails were complemented by ground-based microphones. Figure 19 shows predicted *6/rev* pilot seat and main transmission vibration reduction for single and multi-harmonic IBC inputs at 120kts. The numbers were computed using T-matrices that have been identified off-line from flight test data. The figure shows vibration reduction of up to 100% for the individual stations. Similar results were computed for the other sensor stations. The IBC inputs were optimised for single sensor stations. Simultaneous vibration reduction at more than one sensor station will reduce the max. achievable vibration reduction. Nevertheless, this is a promising result. The IBC amplitudes for all harmonic combinations added were well below 1.1°, although frequency combinations require higher amplitudes than single harmonic IBC inputs. This campaign revealed the value of *(N_{BL}-2)/rev* control for vibration reduction. For the 4-bladed Bo 105 *2/rev* IBC was very helpful to reduce vibrations. The same turned out for the 6-bladed CH-53G using *4/rev* IBC, especially in combination with other frequencies. BVI noise was reduced through *2/rev* IBC by 3dB in descent flight at 65kts and -6° flight path angle. The optimal phase was 30° at the controlled amplitude of 0.67°. With full authority of 1.1° 5dB BVI noise reduction should be within reach. The campaign also revealed noise reduction in straight level flight. Furthermore, pitch link load reductions were observed. The pitch link load peak-to-peak value was reduced by 27% at *2/rev* IBC, 0.67° amplitude and 270° phase and by 11% at *3/rev* and 0° phase. Finally, power reduction in high-speed forward flight was investigated using *2/rev* IBC at 0.67° amplitude. Since the flight conditions varied from one data point to the next during phase sweep, the power consumption had to be corrected to eliminate power decrease or increase caused by descent/climb or deceleration/acceleration of the aircraft. The corrected maximum power reduction was about 7% at 125kts and 210° phase.

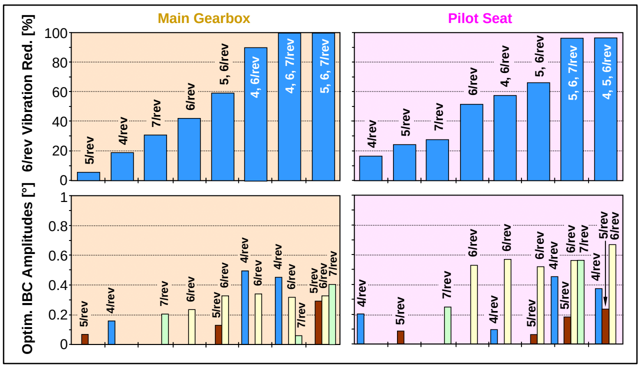

Figure 19: Predicted *6/rev* vibrations at main gearbox and pilot seat for various IBC control laws, 120kts level flight.

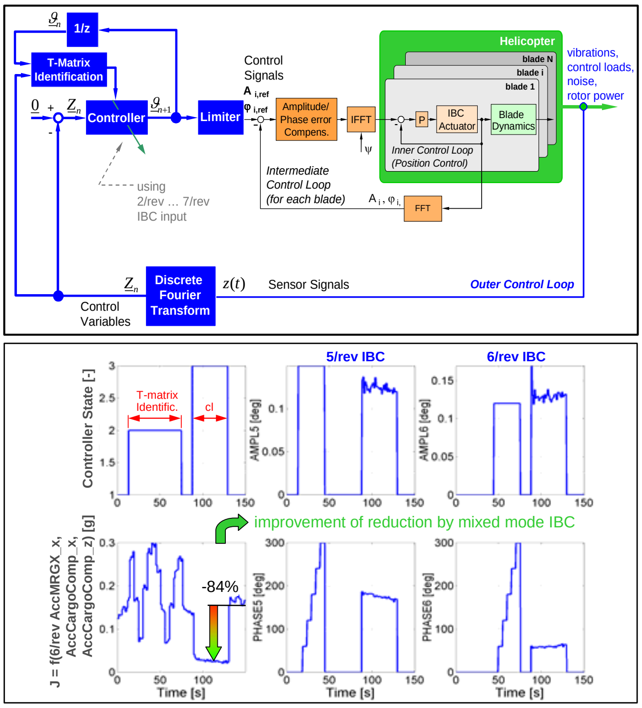

Figure 20: Closed-loop (cl) structure and *5* and *6/rev* cl IBC at 70kts, controlled vibrations: *6/rev* of main transmission x-direction (AccMRGX_x), cargo compartment x- and z-direction (AccCargoComp_x, AccCargoComp_z).

Results of the closed-loop campaign are summarised in [37] and [38]. The control algorithm and the hard- and software installations are outlined in [37]. The control algorithm is based on the linear T-matrix model Figure 20 (top). Non-adaptive and adaptive algorithms for the outer loop were programmed. Main focus was closed-loop vibration reduction at various accelerometer locations using single and multi-harmonic IBC in steady state and manoeuvring flight. Figure 20 (bottom) shows an example of *5* and *6/rev* IBC to minimize vibrations at main transmission and cargo compartment and two different spatial orientations. After identifying both T-matrices 84% reduction of the cost function was achieved. Vibration reduction in two different flight manoeuvres is shown in Figure 21. The controller was updated every fourth rotor revolution. The time histories show that the peak accelerations in the sensor signal (orange ellipses) of the reference open-loop trial were cancelled with IBC. Similar results were gathered for turns. In addition the controller was also applied to minimize *2*, *3* and *4/rev* harmonics of the pitch link load by *2/rev* IBC. The peak-to-peak values were reduced by 30% at a controlled amplitude of 0.9°.

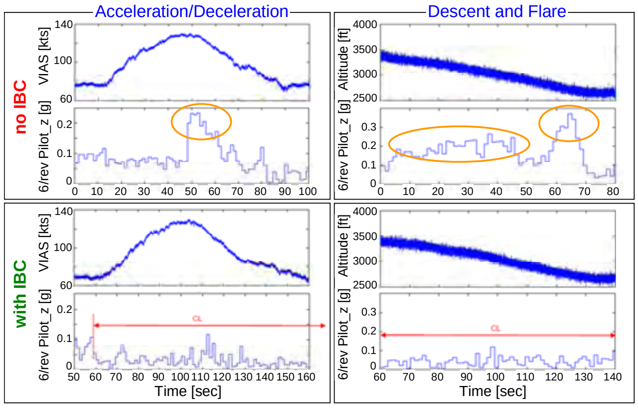

Figure 21: Open- and closed-loop *5/rev* IBC during manoeuvres, controlled vibration *6/rev* pilot seat, z-direction.

Testing of an IBC system on a full-scale UH-60 rotor was performed in the 80x120ft² and the 40x80ft² Ames wind tunnels in 2001 and 2009[3]. Figure 22 shows the large rotor test apparatus (LRTA) and the IBC system. The standard bifilar absorbers were removed.

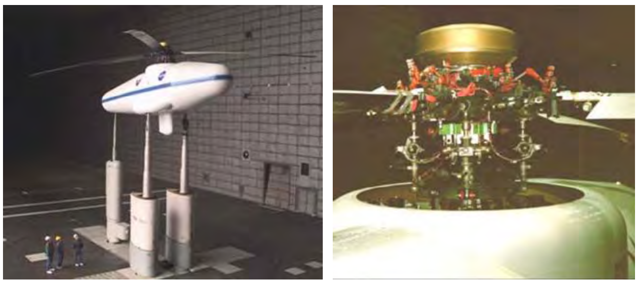

Figure 22: UH-60 rotor and LRTA in the 80x120ft² wind tunnel and close-up view on the IBC system.

The IBC actuator had an authority of up to 6° blade pitch angle at low IBC frequencies and 1.6° at *7/rev*. Details on hardware, instrumentation, data acquisition etc. of the 2001 campaign in the 80x120ft² wind tunnel can be found in [39]. The instrumentation covered blade strain gauges, blade accelerometers, blade pressure transducers, hub-mounted gauges for stress monitoring, LRTA balance data, 16 microphones in the wind tunnel (8 on a traverse) etc. Results gathered during the first test are presented in [40]. BVI noise and vibration reduction were addressed. For vibration reduction the advance ratio μ, blade tip Mach number, shaft angle, pitching and rolling moments and blade loading C_T/σ were chosen to match a free flight condition. Trim was maintained during IBC. For noise reduction, advance ratio μ, blade tip Mach number, shaft angle and blade loading C_T/σ were set to the desired test conditions and cyclic trim was used to minimize *1/rev* flapping. The most pronounced vibration condition was at 46kts (μ = 0.1) and C_T/σ = 0.0725. The most effective frequency in reducing *4/rev* vibrations was *3/rev*. It reduced vibrations at

[3] Partners were NASA, US Army, Sikorsky and ZFL

1° amplitude and 315° phase by 70%. No drawback on other vibratory frequencies was observed. The second best frequency was *4/rev*, *2/rev* was less effective, but was again important for BVI noise reduction. Test conditions were 4° and 7° aft tilt of the rotor shaft at 75kts (μ = 0.16) and C_T/σ = 0.09. A *2/rev* amplitude of 3° achieved at 190° phase angle a BVI noise reduction at the advancing side of 6 to 8dB. The same amplitude at 180° phase angle reduced BVI noise at the retreating side (two microphones in the fourth quadrant) by 10dB. This input has an impact on *4/rev* vibrations. While *4/rev* lift vibrations were reduced, shear and moment vibrations were significantly increased. Results gathered throughout the second wind tunnel campaign are presented in [41]. Objective of this second campaign was primarily performance improvement, but also on vibration, noise and load reduction, in-flight tracking and reconfiguration. The instrumentation differed from the previous test, see [41] for details. Ten fixed microphones were used in the tunnel, two under the advancing side, eight upstream ahead of the rotor. Closed-loop IBC was applied. Algorithms were again based on linear T-matrix models. The impact of *2/rev* on power reduction and lift-over-drag (*L/D*) improvement is shown in Figure 23. The chosen flight condition at μ = 0.4 is slightly beyond the UH-60 flight envelope. At a phase of 225° and about 2° amplitude 5% power reduction was achieved. This corresponds to 8.6% *L/D* improvement. Larger amplitudes do not improve both values.

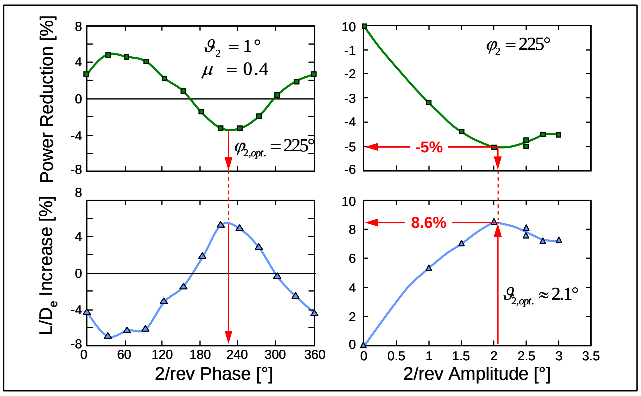

Figure 23: Power reduction and lift-over-drag improvement using *2/rev* IBC, μ = 0.4.

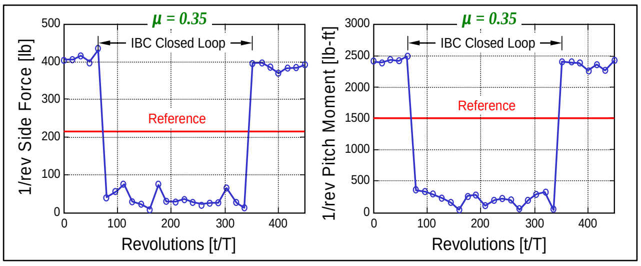

Figure 24: Closed-loop reduction of selected *1/rev* balance loads, incorrect balance weight.

The findings with respect to the pitch link load reduction were similar to the CH-53G flight tests. The peak-to-peak values were reduced by 20 to 30%. The tests also revealed an impact of *3/rev* IBC on in-plane noise reductions, but only preliminary results were presented. Finally, in-flight tracking results were presented. Two different defects of rotor blades were simulated, firstly incorrect balance weights and secondly incorrect trim tab setting. An example for incorrect balance weight can be seen in Figure 24. The controller was tuned to minimize *1/rev* side force and pitching moment vibrations using blade pitch offsets of blade 1 and 2. When the controller is active, the vibrations drop below the vibrations of the tracked reference rotor.

Blade root actuation is a straightforward solution to realize IBC. Many aspects have been improved e.g. vibration reduction, BVI noise reduction, performance enhancement, pitch link load reduction and others. Although this IBC concept has demonstrated its reliability and the capability to retrofit existing helicopters, attention was directed more and more towards smart actuation, like active trailing edge flap and active twist. This is due to the immense hardware effort of blade root actuation in the rotating system and associated weight and costs.

2.2. Active Trailing Edge Flap

A survey on vibration reduction by various active rotor control concepts with focus on active flaps is given by FRIEDMANN and MILLOT in [2]. FRIEDMANN updated the active flap technology aspects of the survey in [42].

Early work on active flap IBC goes back to the mid of the 1960s. Although first tests used simple collective and cyclic control to study blade stall delay [43] the results are worth to be mentioned. The 2-bladed rotor with 12m diameter did not include feathering bearings. Flaps extended from 0.7R (R = rotor radius) to the tip. The rotor featured a jet drive. Compressed air was ducted through the blades and exhausted through nozzles in front of the flaps. This provided the torque. The flaps were mechanically deflected causing the jet flow to follow the upper flap surface by the Coanda effect. The rotor was tested in the 40x80ft² NASA Ames wind tunnel at advance ratios of up to 0.5.

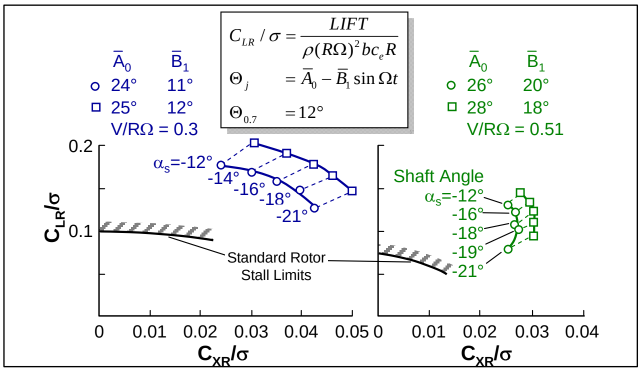

Figure 25: Jet-flap rotor force capability, Θ_j = jet deflection, $\Theta_{0.7}$. = collective pitch at 0.7R.

At μ = 0.3 and 0.5 the jet-flap rotor showed a significant capability to generate lift (shown as rotor lift loading C_{LR}/σ) and propulsive force (shown as rotor propulsive force loading C_{XR}/σ), Figure 25. The retreating blade stall limit of conventional rotors is shown, too. The load capability of the jet-flap rotor is 2 to 2.5 times the capability of a conventional rotor. The trailing edge flap-control used here was a pure collective plus *1/rev* part and might be interesting for swashplateless rotors. In a further study McCLOUD and KRETZ explored the capability to alleviate blade stress and vibrations [44]. In addition to collective and *1/rev* cyclic control, the flaps now also provided *2*, *3* and *4/rev* harmonic variations. This reflects the idea of active flap IBC, but was called multi-cyclic control. It is worth noting that the T-matrix approach has been developed in the context of the jet-flap rotor tests. The transfer-matrices were determined from experiments. Then optimal control vectors and stress or vibration vectors were calculated. This approach reduced *2nd* to *4th* harmonics of blade bending stress, but on the expense of increased *1/rev* stresses and hence rotor trim. The T-matrix approach was also applied to improve root-mean-square (RMS) stress. Reductions of 40% to 66% were calculated. Next, *2nd* and *4th* harmonics of vertical vibration content were addressed using *2/rev* and *4/rev* flap deflections. Theoretical analysis revealed an increased *3rd* harmonic blade stress. On the other hand, RMS control turned out to sometimes increase vibrations.

In 1976 full-scale wind tunnel testing was conducted in the NASA Ames 40x80ft² facility using a multi-cyclic twist control rotor (MCTR) manufactured by Kaman [45]. The 4-bladed MCTR used servo-flaps aft of the trailing edges to control collective flap deflection and *1* to *4/rev* flap deflection. The four electro-hydraulic flap actuators were located in the hub. Main interest was the measurement of vibrations, power, blade bending moment etc. and to derive these parameters as a function of collective to *4/rev* flap deflections. The range of control was limited to ±5° for each harmonic and the resultant maximum deflection for *2* to *4/rev* was ±8°. Multi-cyclic control achieved significant reductions in blade bending moments and blade actuator control loads at various flight conditions. Higher harmonic terms of servo flap actuation were found to also modify the transmission vertical vibrations and pitch link loads.

MILLOT and FRIEDMANN [46] were the first to use aeroelastic simulation for investigating vibration reduction by trailing edge flaps. A first feasibility study was based on an offset-hinged, spring-restrained, rigid blade model undergoing coupled flap, lag and torsion motions. Modified quasistatic Greenberg theory was used for the aerodynamic loads. Reverse flow was considered. Inflow was assumed to be constant. Controller designs aimed to minimize a quadratic cost function that included vibrations, control inputs and their variations. Two T-matrix models were used: a global and a local model. The T-matrix of the global model was assumed to be independent of the control input. The second used a linearised vibratory hub load response to control about the current value of the control vector. Baseline was a 4-bladed helicopter at an advance ratio of 0.3. The flap size was 25% in chord, 20% in span, centred at 75% radius. Control harmonics covered *2/rev* to *5/rev*. Figure 26 shows vibration reduction potential of blade root IBC and flap IBC for two different torsional frequencies for the local model. Blade root and flap IBC achieved similar results. Torsionally soft blades were mentioned to support vibration reduction and to lead to reduced control amplitudes. Actuation power of blade root IBC was four to eight times higher than with the active flap. This gap even increased when fully flexible blade models were used [2].

The flexible blade formulation was improved to include compressible time domain unsteady aerodynamics and free wake. Since piezo-driven flaps might run into saturation, ref. [47] applied three methods to alleviate this problem: 1) clipping of the optimal flap deflection, 2) down-scaling of the flap input and 3) iterative adjustment of the control weighting matrix of the cost function until flap deflection was properly constrained. These methods were compared to unconstrained flaps. The unconstrained control resulted in flap deflections that were beyond actuator capabilities and clipping and down-scaling resulted in poor vibration reduction. Iterative weighting led to sufficient vibration reduction at limited actuator requirements. Single and dual active flaps to reduce dynamic stall-induced vibrations were investigated in [48] using the Onera dynamic stall model. Freeplay of the flaps was also considered, but was found to have moderate impact on the vibration reduction.

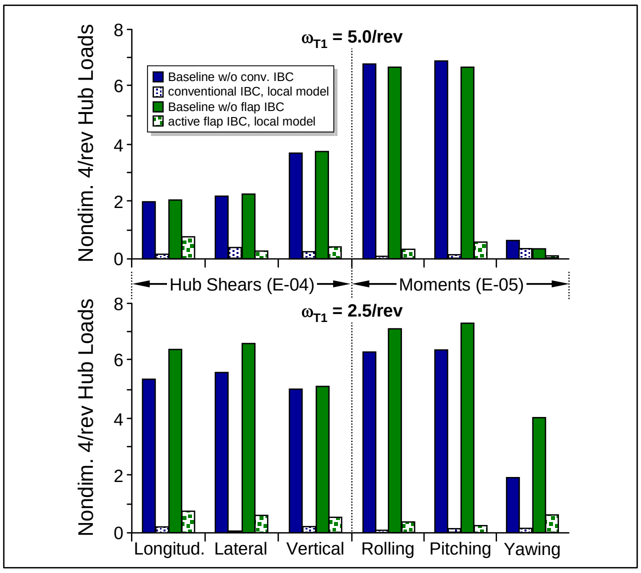

Figure 26: Vibration reduction, comparison of blade root IBC and active flap IBC.

Ref. [49] investigated the impact of reducing BVI-induced vibrations on rotor noise. The aerodynamic rotor code was capable of computing unsteady time-domain blade surface pressure distributions and included effects of compressibility and free-wake. This code was coupled to an aeroelastic flap-lag-torsion blade model. Acoustic predictions were based on the WOPWOP tool. The code was validated with HART (Higher Harmonic-Control Aeroacoustic Rotor Test, see [1]) data. Flap harmonics covered *2/rev* to *5/rev*. Single and dual flap configurations were considered on a helicopter representing the Bo 105. The dual flap was more efficient in reducing vibrations and did not change the noise levels. The single flap showed a slight drawback regarding the BVI noise footprint. To prove simultaneous noise and vibration reduction with active flaps, a second study was conducted with an improved free wake model [50]. The T-matrix formulation was applied to relate *4/rev*-vibrations and BVI noise harmonics (*6th* to *17th* blade passage frequencies) to the control inputs. Noise levels were computed for a feedback microphone on a boom extending from the right landing skid at the rear. Simultaneous noise and vibration reduction was achieved for single and dual flap configurations constrained to 4° authority. The dual flap (40% vibration and 5dB advancing side noise reduction) was more efficient than the single flap. Due to the microphone position, a slight increase of 1dB of the retreating side noise was discovered.

A recent study focussed on performance enhancement and vibration reduction [51]. The simulation code was based on the model presented in [48]. Again, *2/rev* to *5/rev* harmonics were considered for single and dual flap configurations. A quadratic cost function of input and output vectors was minimized. The output vector included the *4/rev* hub load vibrations of a Bo 105-like[4] helicopter as well as the averaged power. Flap authority was limited to 4°. The adaptive control algorithm could reduce power at μ = 0.35 and C_T/σ = 0.0714 by 1.73% (single flap) to 1.76% (dual flap) at deflections of less than 3°, but increased vibrations. The optimised flap input included the *2/rev* harmonic and a large *3/rev* contribution. Considering both objectives simultaneously, power reductions got worse (far below 1%) while reducing the vibrations by 68% for the single flap configuration. The dual flap was less effective. Conventional blade root IBC achieved similar results. Higher power savings were computed at higher C_T/σ and at μ = 0.4, but reduced blade loading.

A comparison of leading edge slat, variable nose droop, oscillatory jet, Gurney flap, blade root IBC, active twist and trailing edge flap with respect to rotor performance improvement is presented in [52]. CAMRAD II with free-wake, but without dynamic stall model was used. The trailing edge flap and active twist were actuated at *1* and *2/rev* and blade root IBC at *2/rev*. Different amplitudes were applied. The other four concepts followed a discrete control scheme. They were activated over a segment of azimuth (i.e. 60° azimuth interval), see [52] for more details. Except for blade root IBC and active twist various different radial stations (inboard: 0.28-0.5R, mid-span: 0.5-0.75R, outboard: 0.75-1.0R) of the control surfaces were considered. The baseline helicopter was a modified AH-64 with VR12 airfoil. For the trailing edge flap, performance improvement turned out to be negligible. Using *2/rev* IBC, active twist and blade root IBC were found to improve power by 2.7% at 150kts. The leading edge slat improved thrust when extended at the retreating rotor side without power benefits. Similar results were obtained with the remaining devices.

Rotor power enhancement is a valuable IBC application, no matter which actuation concept is preferred. However, the practical application may be problematic due to challenges in precise measurement of rotor power or rotor torque. This is less important for wind tunnel tests or aeroelastic simulations, but it is important for free flight conditions. The power consumption is very sensitive to variations in the flight condition (deceleration/acceleration, climb/descent, …). And any power reduction through IBC might be covered by changing flight conditions. A closed-loop control system would have to take this into account. This was outlined in [36]. The answer to that question is rather important from a system engineering point of view.

Simulation codes are valuable means to get insight into various phenomena of active rotor control. FRIEDMANN [42] points out that aeroelastic simulation codes capable of modelling vibration reduction using trailing edge flaps have to be rather refined to provide the level of accuracy required for correlation with experimental data and validation with experimental data itself would be a necessity.

A 7.5ft diameter 2-bladed hingeless rotor model with trailing edge flaps was investigated in [53] to [55]. The flap (10% chord, 12% radial span and centred at 0.75R) was driven by piezo-ceramic bimorph actuators with ±5° flap amplitude at nominal rpm of 760rpm. Primary objective was to explore the dynamic characteristics of such a rotor. The rotor was operated in the first tests in hover condition at several rotational speeds. A simple 2-DOF model undergoing rigid blade flap and torsion was presented and compared to the measurements. Low-frequency blade root torsion moment response to flap deflection was found to increase with rotor speed. Low-frequency blade flap bending moment response to trailing edge flap deflection was found to increase due to direct lift effect as the rotor was speeded up, but than decreased due to an opposing torsion effect caused by the flap deflection. This led to “flap reversal” slightly above nominal rpm. The rotor was tested in a second campaign from μ = 0.1 to 0.3 at low to moderate thrust coefficients [54]. This test also investigated open-loop vibration reduction benefits. The trim procedure minimized the *1/rev* blade flap bending moment by cyclic pitch. The test revealed the possibility to control flap bending moments by *1* to *5/rev* trailing edge flap deflections. An amplitude of ±5° turned out to be sufficient at the individual control frequencies to cancel the blade bending harmonics at appropriate phases except for *2/rev*. However, this increased torsion moments. Ref. [55] gives more insight into the dynamics of a blade-flap system. Two models were presented, the rigid blade model of [53] and a more refined elastic finite element model for flap, lag and torsion using constant uniform inflow as well as unsteady 2D aerodynamics according to Theodorsen’s theory. Emphasis was on to the investigation of the flap efficiency at various rotor operating conditions. The trailing edge flap reversal was explained as a phenomenon that occurs when rotor speed increases to the point where the lift produced by flap deflection (direct lift, described by $c_{l\delta}\ \delta$, δ = flap deflection, $c_{l\delta}$ = airfoil lift derivative due to flap deflection) is overcome by the opposing lift associated with elastic twist induced by the pitching moment of the trailing edge flap (captured by $c_{l\alpha}\ \vartheta$, ϑ = torsional deflection, $c_{l\alpha}$ = airfoil lift slope). Both models matched experimental data well and could predict the trailing edge flap reversal speed. Parametric studies with the second model revealed that benefits on vibration reduction can be achieved by lowering the torsion stiffness of the blade and for the first torsion eigenfrequency close to the frequency of the *2nd* blade flap mode.

A different flap actuation design is proposed in [56]. A two-bladed model with 1.83m diameter was built and hover-tested. The actuator was a composite beam with piezo-ceramic elements bonded to the upper and lower surfaces. Proper design converted the bending-torsion coupled beam in a pure twist actuator. The induced tip twist of the beam deflected the flap. The flaps (20% chord and 3% span, centred at 90% radius) were directly connected to the beam. Rotor speeds from 300 to 900rpm (M_{Tip} = 0.25) were tested and *4/rev* deflection amplitudes of 1.5° to 2° were achieved at excitation levels of 50% of the piezo limits.

[4] A NACA 0012 airfoil was used instead of the original NACA 23012.

Cancelling vibrations caused by rotor blade dissimilarities was investigated in [57], [58]. The first reference is a numerical investigation based on a 5-bladed MD 900 and proposes an adaptive algorithm using the T-matrix relation:

$$Z_i = Z_{i0} + T_{ij}\delta_j$$

where Z_i now was defined as the vector of the hub loads (F_x … M_z) sampled over one rotor revolution at N_s points, Z_{i0} as baseline vibration vector and δ_j as vector of the five individual flap deflections. This control approach was compared to the classical one which uses the same, but azimuthally shifted inputs for all flaps. Two sources for rotor dissimilarities were studied: mass imbalance and differing nose-down pitching moment coefficient for one blade section. The mass damage introduced large *1/rev* shear forces (F_x and F_y). When controlled simultaneously, the hub loads were reduced by just 40%. This was caused by limiting the flap deflections to ±4°. The aerodynamic fault caused *1* and *2/rev* hub moment variations (M_x and M_y) and *1/rev* vibrations in vertical shear. When controlled simultaneously, the hub loads were reduced by more than 70%. The new control approach was regarded as superior to the classical one. This work was continued in [58] using a 4-bladed rotor on a hover test rig. The flaps were driven by piezo-electric benders. The hub was a 1/7 scaled Bell 412 bearingless hub. The *1/rev* vibratory loads were generated from inherent blade dissimilarities and imperfect trim. The individual flap deflection approach of [58] was compared to the classical approach. Figure 27 shows reduction of *1/rev* vertical hub shear force for both control concepts. The individual controller (bottom) is efficient in reducing these vibrations by 90% at small flap deflections, while the classical one (top) is not.

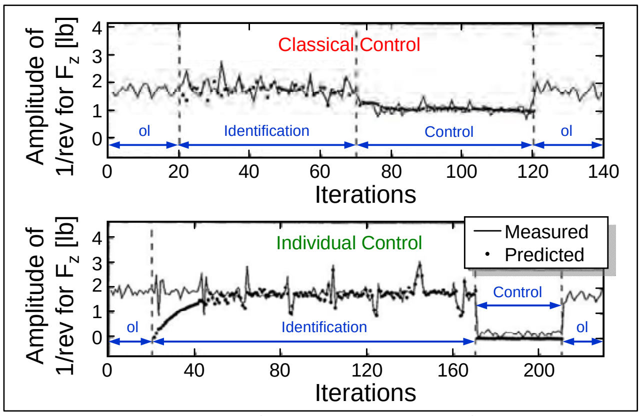

Figure 27: Reduction of *1/rev* hub vertical force using individual (bottom) and classical control (top).

The effects of HHC and active flap actuation on BVI are compared in [59]. Wind tunnel tests were conducted with a one-bladed rotor of 1m radius and rectangular blade planform at tunnel speed V_W = 20.1m/s and 600rpm. Both control techniques used *2/rev* control, HHC at 2°, the flap at 6°, 18° and 24° amplitude. The flap was 25% in chord stretching from 80% to 98% radius. Blade vortex miss-distance was measured by Laser Light Sheet technique on the advancing side. A maximum blade vortex distance was achieved for HHC at 80° (vortex below blade) and 160° (vortex above blade) phase[5], see Figure 28. Using the active flap, larger flap angles resulted in larger noise reductions. A drive torque index to control the blade pitch by HHC or a flap was introduced. It showed advantages of the active flap over HHC. This indicates the larger effort to rotate the whole blade (for HHC) instead of a "small" flap with low inertia (for active flap control).

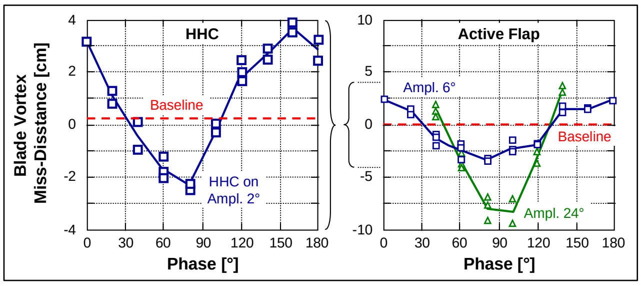

Figure 28: Blade vortex miss-distance using *2/rev* HHC and active flap, 600rpm, V_W=20.1m/s, collect. pitch Θ_0=5°.

Full-scale whirl tower testing of a rotor featuring HHC and an active flap is presented in [60]. Rotor radius was 5.8m. Three flaps were manufactured with 10%R in span and 10, 15 and 20% in chord. The flaps were centred at 75%R. They were driven by two piezo-ceramic actuators and featured a Kevlar cloth solid state hinge. Limited flap deflections for both wider flap chords resulted from actuator limitations and increasing flap actuation power with increasing flap chord. An improved rotor design with modified flap actuation is presented in [61]. The paper first summarizes theoretical studies on the impact of flap chord, span and position on flap efficiency that led to a requirement for sufficient BVI reduction. This was 6° flap amplitude at *2/rev* for a 10% chord, 10%R flap centred at 75%R. The design is shown in Figure 29. It features two actuators that work in push-pull mode. The hinge is again a composite hinge. A 1m blade segment with integrated flap was tested in a transonic wind tunnel at Kawasaki Heavy Industries Ltd. [62]. For *2/rev* input the achieved flap amplitude was 6° in BVI and 3.8° at high-speed condition. Control of *3* to *5/rev* led to 5.7 to 5.8° flap amplitudes at the BVI condition.

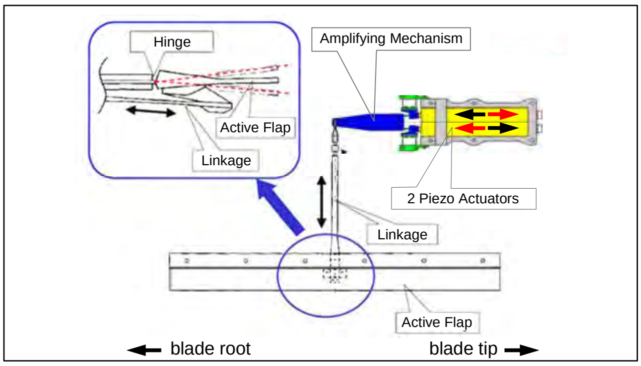

Figure 29: Flap actuation concept.

Wind-tunnel testing of a 4-bladed articulated rotor with different radial flap positions was conducted 2005 in the transonic Onera S1 Modane wind tunnel [63] as a result of an Onera-DLR cooperation. Main objectives were BVI noise and vibration reduction as well as performance improvement. The rotor featured 4.2m diameter and three different radial flap positions ranging from either 0.69R to 0.79R, 0.75R to 0.85R or 0.8R to 0.9R. The inboard posi-

[5] Please note: the phase definition differs from that of [1].

tion was intended for vibration, the outboard position for noise reduction. The flap itself was 15% in chord. Piezo-electric actuators were used to drive the flaps. Blades were equipped with pressure transducers, strain gauges and the hub with accelerometers (in total 300 rotating sensors). Fourteen fixed microphones were used for noise measurement. The rotor was designed as a Mach-scaled rotor. However, the operating speed of 980rpm was reduced to 800rpm. This was caused by the proximity of a flap-torsion mode to the *4/rev* rotor harmonic. Nevertheless, noise reduction in BVI condition has been demonstrated. An example is shown in Figure 30 for *4/rev* flap actuation.

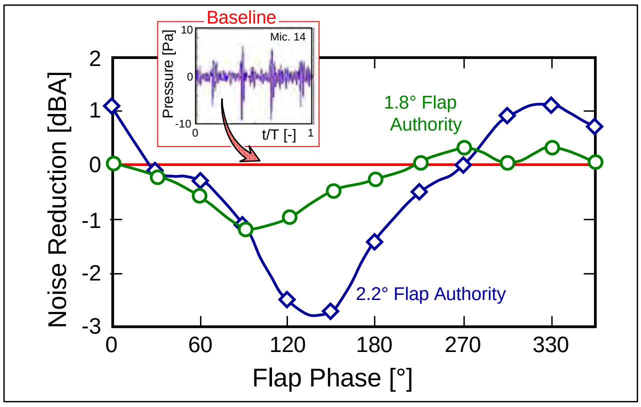

Figure 30: Noise reduction in BVI flight condition by *4/rev* flap actuation, μ = 0.22.

Also shown in the figure is the filtered pressure fluctuation of microphone no. 14 (located underneath the advancing side). It depicts BVI related fluctuations. Larger flap amplitudes led to higher noise reductions (-1.2dBA to -2.7dBA). More reduction should be expected for *2/rev* IBC. Yet, the results must be taken with some care since the test was not explicitly devoted to noise measurements and the radiation directivity characteristics may have biased these results.

First flight testing with an active trailing edge flap rotor has been conducted by Eurocopter in 2005. The 4-bladed demonstrator based on a BK 117 (main rotor radius = 5.5m, TOW = 3to) and is shown in Figure 1 (middle). The design process of the blade-flap system is described in [64]. Objective of the project ADASYS (Adaptive Dynamic Systems) was to demonstrate noise and vibration reduction by means of trailing edge flaps. *2/rev* control was intended for noise, *3*, *4*, and *5/rev* for vibration reduction. Attention concentrated on the aeroelastic and dynamic characteristics of the blades. CAMRAD II was used to design the flap (radial position, chord, span). The flap size was 15.6% in equivalent chord and 10.9% in span. The ADASYS rotor is based on the EC 145 rotor and can be equipped with up to three different flap units at 71.8%, 77.3% and 82.7% radial station. The torsional frequency of the blade was lowered (*4.3/rev* for standard EC 145) to approx. *3.5/rev*. This supports the servo-effect of the flap. The standard blade pendulum absorbers were removed. The first flight tests confirmed the capability of the flap to alleviate fuselage vibrations. More information on the demonstrator itself is given in [65]. For noise reduction the flap should be positioned as close as possible to the blade tip. Due to the swept back tip this requirement was almost achieved by the outermost flap station while the most beneficial flap location for vibration reduction was in the mid span range at 73%R. This was nearly satisfied by the innermost flap. Each flap was driven by a pair of piezo-electric actuators. The actuator-flap system was integrated into a flat carbon fibre box that can be inserted into the blades. Maximum flap angle was ±10°. The same disturbance rejection method as for the Bo 105 [34] was applied for vibration reduction. The concept was tested in level flight (50 – 110kts, rpm variations 98% - 102% at 100kts), climb/descent (±1500ft/min at 65kts) and manoeuvring flights (left and right turns at 50° bank angle and 80kts). The controller performed well throughout all flight tests. Figure 31 shows vibration reduction results in level flight at the gearbox and the cabin (left). The three controlled hub loads are shown on the right hand side. Although the controller has been designed for 100kts, the vibrations were reduced for the entire speed range. Again, the remaining accelerations can be explained by the non-controlled hub loads. This shows that vibration reduction via flaps is as powerful as by blade root IBC.

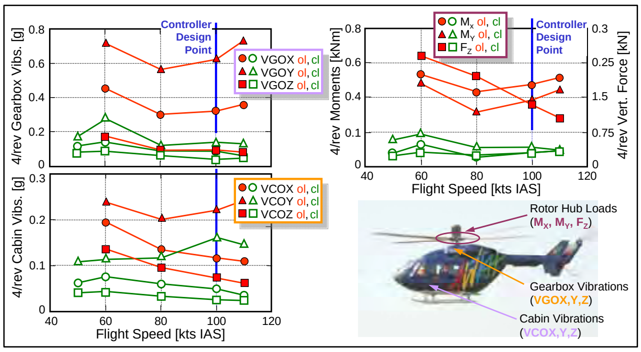

Figure 31: *4/rev* vibrations at gearbox (VGO) and cabin (VCO) in level flight versus speed, 100% rpm.

In the demonstrator aircraft main components were located on the top of the rotor hub. This bulky system contains communication and power electronics. It causes much drag and limits maximum speed of the test bed. Current work, therefore, intends to reduce volume and weight of the electronics to allow installation below the cap of an EC 145 rotor. Further research focuses on the reduction of the actuator weight and increasing reliability by replacing the amplification metal frame of the piezo-actuator by a fibre composite one.

Recently, wind tunnel testing of the 5-bladed bearingless MD 900 SMART rotor with active trailing edge flaps has been conducted in the 40x80ft² Ames wind tunnel[6]. A summary of the results is given in [66], while [67] and [68] focus on BVI and in-plane noise aspects, respectively. Objectives were noise and vibration reduction as well as control power, blade tracking and performance enhancement. The flap was 25% in chord (with 40% overhang giving a total length of 35% chord), 18% in span and centre at 83% radius. Flap actuation was mechanically limited to ±6°. First torsional frequency of the SMART rotor was not changed compared to the baseline rotor (i.e. *5.8/rev*). Each blade was driven by two X-frame actuators. Figure 32 shows the rotor and details of the actuator. Maximum control frequency was *11/rev* with as much as 4° flap angle.

[6] Partners were Boeing, NASA, US Army, DARPA, MIT, UCLA and Univ. of Maryland

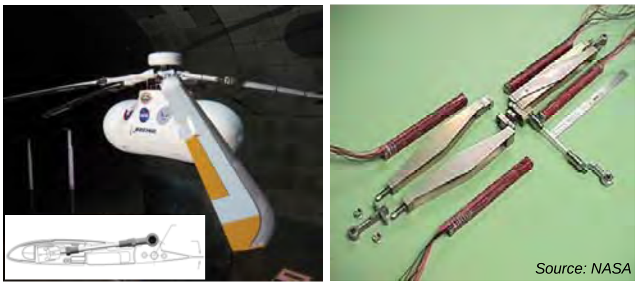

Figure 32: SMART rotor in the 40x80ft² wind tunnel and X-frame actuator.

Blade loads were measured at various radial blade stations. Pitch link load and shaft torque were measured also. Hub accelerations, static mast bending, rotor balance data etc. were measurements of the test stand. A series of microphones were used for noise measurements, see [67] and [68] for details. The rotor was set to the desired thrust (C_T/σ = 0.075) and minimum flapping was trimmed. Retrim was not always conducted. Although a rather large flap was used and torsional frequency was quite high, the flap turned out to act via the servo effect. Highest noise levels were measured at μ = 0.15, α = +4°. In this condition BVI noise reduction turned out to be most effective for 1.5° flap amplitude and 30° phase at *4/rev*. Traverse sweeps without and with active flap are shown in Figure 33. Noise reduction was as high as 7dB and at the hot spot location (i.e. location of highest noise level) 3.5 to 6dB. However, this flap actuation increased vibratory hub loads. At the more important FAA noise certification point (μ = 0.165, α = +1.8°) *3/rev* at 1.5° and 180° phase was most effective and could reduce BVI noise at the hot spot by 3 to 5dB. This is noticeable, since most literature mentions *2/rev* to minimize BVI noise best and might be explained by the high torsional stiffness. It should also be noted that the hot spot with active flap has been shifted slightly outside the area covered by the traverse sweep. The phase of this reference is shifted with respect to the one in [1] by -90°.

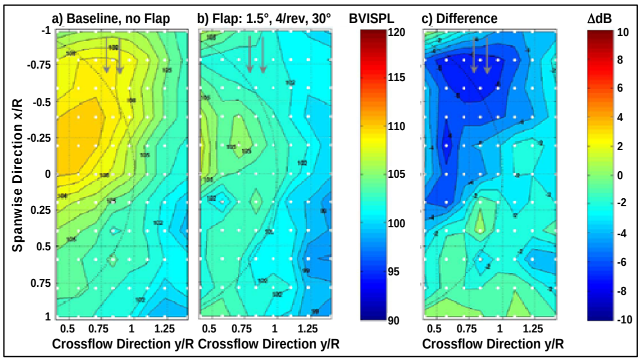

Figure 33: Traverse sweep at μ = 0.15, α = +4° without and with active Flap.

Ref. [68] outlines the effect of reducing in-plane noise. Two noise sources are mentioned to contribute to low-frequency noise of modern helicopters: thickness noise (moving the blades through the air) and loading noise (generation of lift). The latter can be divided into out-off- and in-plane noise. The presence of thickness and in-plane loading noise offers the chance to alter in-plane loading noise by IBC such that both sources cancel each other (Figure 34, top).

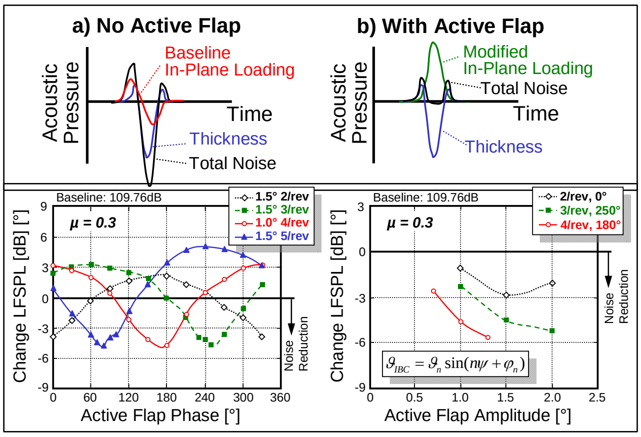

Figure 34: In-plane noise reduction principle (top) and in-plane noise (low frequency sound pressure level, LFSPL) reduction, μ = 0.3, α = -9.1° (bottom).

Figure 34 (bottom) shows low-frequency (first six blade passage frequencies, i.e. *30th* harmonic) sound pressure level reductions. Again, *4/rev* turned out to be very valuable and reduced noise by 5.7dB at 1.3° amplitude and 180° phase. Second best was *3/rev* with 5.1dB reduction at 2° amplitude and 250° phase. Again, noise reduction was accompanied by an increase in *5/rev* in-plane hub loads. With respect to vibration reduction *4/rev* turned out to be very and *6/rev* least effective. While most literature focuses on the reduction of the lowest blade-number harmonic (i.e. N_{BL}/rev) in the fixed frame, in this test e.g. *1* to *5/rev* were also considered for the controller design. Using such a controller the first five harmonics of the normal load were almost completely eliminated at high speed (μ = 0.3, α = -9.1°) and in descent (μ = 0.2, α = +2°). At both flight conditions the reduction was as high as 95%. Control of vibratory rolling moment in descent and pitching moment in level flight was more difficult. The first five harmonics were reduced by 68% and 73% respectively.

The losses in the amplification system of smart actuators and the penalty incurred in adding the mass of the actuator-flap-unit aft of the 1/4 chord line are disadvantages of active flaps [56]. Another drawback is the drag and hence power increase associated with flap deflection. A value of 2% is mentioned in [42]. Regarding power, all active control concepts have to be carefully evaluated against each other. Deflecting the control surface (the flap or the whole blade as for HHC/IBC) consumes power, too. Rotor dynamic tuning might also become more difficult [55]. Compared to blade root IBC active flaps offer advantages in safety [64], since the actuators are no longer integral parts of the primary control system, complexity (electrical instead of hydraulic power) and weight.

2.3. Active Twist

Even more advanced is active twist actuation. One advantage of such a system is the elimination of mechanical hinges, bearings or stroke amplification resulting in no wear. Active twist does not use local concentrated actuators and offers new applications like twist optimisation for hover and forward flight, if sufficient twist can be generated. On the other hand this concept requires a large number of distributed smart elements to generate a sufficient blade twist. This causes a significant weight penalty and an increase in blade stiffness from its baseline value [3]. Also, cost is an issue for such rotors since a large quantity of smart material is used. The costs may go down in the future, if other industry sectors such as the automobile industry increase the use of these materials. With respect to the twist requirements, lessons learned from the Bo 105 flight tests give valuable clues. The reason for the success of those flight tests (see [28] to [34]) was seen in the excitation of the first torsion mode by the IBC system [64]. Although the IBC amplitude was only about 1° (hard stops at 1.1°), the computed blade tip deflections were much higher, depending on the harmonic excitation. At *2/rev* the blade tip pitch angle was about 1.4°, 2.1° at *3/rev* and 2.2° at *4/rev*. If by active twist similar tip deflections can be achieved, this will support successful IBC applications. Similar requirements were mentioned in [69].

Early work on active twist rotor blades was done at the University of Maryland. CHOPRA [69] summarises some of this work. A smart 6ft 2-bladed, bearingless, 1/8-Froude-scaled rotor was manufactured. Blade length was 26.85in (68.2cm) and chord was 3.0in (7.62cm). Five discrete piezo-ceramic elements manufactured from 9.5mil (0.24mm) thick G-1195 crystals were embedded under the fibreglass skin in banks at ±45° orientation on the top and bottom surface of the blades. Since torsional stiffness turned out to be much too high for a Froude-scaled rotor, tip twist amplitudes were low. A non-rotating static tip twist of 0.15° and a dynamic tip twist of 0.1° in hover at *4/rev* excitation and operating speed were achieved.

Ref. [70] summarises results of a two-phase project between Boeing, MIT and Penn State University. Within phase I two smart blades (basis: 1/6-Mach-scaled CH-47D) were manufactured, tested in hover and compared to each other. The first used a trailing edge servo-flap (driven by a X-frame actuator), the second active twist (the actuation system used active piezo-fibre composites, AFC). The active fibres were placed within the upper and lower laminates of the blade spar. It turned out that the piezo-twist blade was easier to design and less costly than the active flap blade. The reason for this was twofold. The active twist blade used integrated actuators which became part of the blade structure and induced its twist directly on the blade. An active flap needs a secondary structure and it requires dynamic pressure to produce a twisting moment. Both aspects increase design complexity and costs. For phase II, the active twist concept was initiated as Active Materials Rotor (AMR). The AMR was a 3-bladed 1/6-scale rotor with advanced design (swept tapered tip, non-linear twist, …). A D-spar of 35% chord with two piezo-plies each on upper and lower surface was selected. First torsion eigenfrequency was about *3.8/rev* (*4.5/rev* for traditional blade). Each ply was made from several piezo patches butted together and oriented at ±45° to the spar. The aim was to reduce 50% of *3/rev* vibrations at various forward flight conditions. Figure 35 shows predicted and measured tip twist in hover. Prognoses revealed that the AMR should reach or exceed the vibration reduction goal.

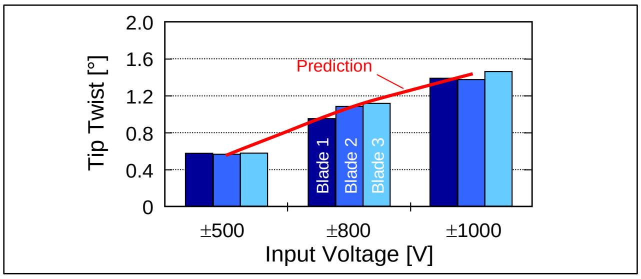

Figure 35: AMR measured and predicted tip twist at hover out of ground effect, *3/rev* excitation at 1300rpm, collective pitch: $\vartheta_{0.75} = 8°$.

Recent research efforts focused on the scaling of this technology up to the requirements of a full-scale heavy lift rotorcraft (CH-47). Objective of this work was to achieve a quasi-static actuated tip twist of an active twist rotor blade of ±2° (4° peak-to-peak) [71]. A 72" (182.88cm) long blade section with embedded AFC actuators was manufactured and tested. The data gathered with this blade segment at low actuation frequencies showed lower induced deformations than expected. An inspection of the blade segment revealed some hardware problems with the actuator packs. Nevertheless, it was concluded that a full-scale active twist blade can be built within the weight limit of a passive blade while providing significant actuation capability.

A 4-bladed, articulated, aeroelastically-scaled Active Twist Rotor (ATR) has been tested by NASA, US Army and MIT in the Langley heavy gas wind tunnel [72]. Mach-scaling was provided by the heavy gas. The rotor was 110in (279.4cm) in diameter with rectangular blades. It used 24 AFC patches at six spanwise stations for each blade. The actuators were embedded within the upper and lower parts of the D-spar stretching from 0.3R to 0.98R. They were oriented such that strain was generated at ±45° to the blade axis. First torsional eigenfrequency was about *5.97/rev*. The blades were instrumented with strain gauges for torsion, flap and lag moment as well as with accelerometers for dynamic twist measurements. Tests focussed on vibration reduction by *3, 4, 5/rev* IBC and were performed in level flight and descent conditions applying minimum flap trim (hover tip Mach number $M_{Hover} = 0.60$, rotor lift coefficient $C_L = 0.0066$, 688rpm). At medium speed ($\mu = 0.14$, rotor-shaft angle of attack $\alpha_S = -1.0°$) significant vibration reductions were achieved by *3/rev* and 1000V excitation at 180° to 220° IBC phase. The *4/rev* non-rotating hub forces were reduced by 60% to 90%, pitching, rolling and yawing moments by 90%, 80% and 30%, respectively. The other IBC frequencies were less effective. At high-speed level flight ($\mu = 0.3$, $\alpha_S = -6.0°$) vibration reduction became less effective. Simultaneous fixed-system shear load reduction was not possible. Figure 36 shows dynamic tip twist angle measurements at 157.5° to 225° azimuth. The curves represent the difference to the baseline blade. As shown, twist amplitudes ranging from 1.1° at *3/rev* to 1.4° at *5/rev* were achieved. Closed-loop control of the ATR for reducing vibrations was shown in [73]. The control approach used a modified T-matrix relation expressed in a continuous-time formulation. The control law was designed to reduce *1/rev* and *4/rev* hub normal shears simultaneously. Collective twist at *1/rev* was used to control *1/rev* vibrations and *4/rev* longitudinal and lateral cyclic twist for the *4/rev* vibratory part. The control of *4/rev* normal shear force by cyclic control was motivated by the findings in [72]. This approach worked quite well. The *1/rev* and *4/rev* portions in normal hub shear were significantly reduced. At some test conditions *4/rev* was almost eliminated. Although intended to reduce *4/rev* normal hub shear vibrations all other hub loads were simultaneously reduced for some test cases.

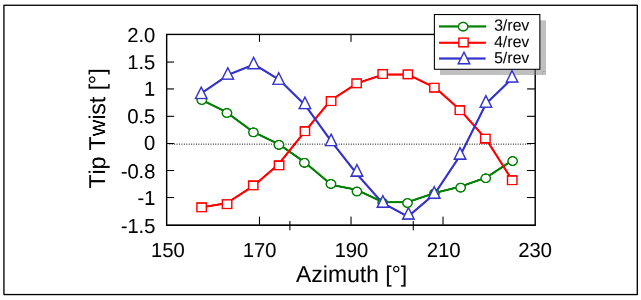

Figure 36: Dynamic tip twist measurement, $\mu = 0.2$, $\alpha_S = -1.0°$, 1000V actuation, control phase 200°.

At Onera and DLR a variety of active rotor blades has been manufactured and tested [74] to [77]. The concepts differ from each other. While Onera follows the TWISCA-concept (TWIstable Section Closed by Actuation), DLR follows an approach which is more comparable to the AMR and ATR blades. It differs in so far as the active fibres are not integrated within the spar, but in the upper and lower skin of the blades. This allows coverage of a larger area by the active material than with spar-integrated active fibres. Both concepts use Micro Fibre Composites (MFC) instead of AFCs. The evolution of the TWISCA concept is outlined in [76]. The TWISCA blade features a slot along the span. The two edges of this slot are bridged via the actuation device. This device induces a relative translation movement in the span direction of the two edges which results in warping of the structure and finally in twisting the blade. The first demonstrators were slotted at the trailing edge. This required the actuators to be placed far behind the 1/4-chord line. A complex balancing concept was required to compensate this and led finally to a rather heavy structure. A second design, therefore, featured a slotted spar (slot at 10% chord). A quasi-static deflection of 1.5° at $1500V_{PP}$ was measured and 2.3° at $2000V_{PP}$ predicted. Sketches of this concept and that of DLR are given in Figure 37.

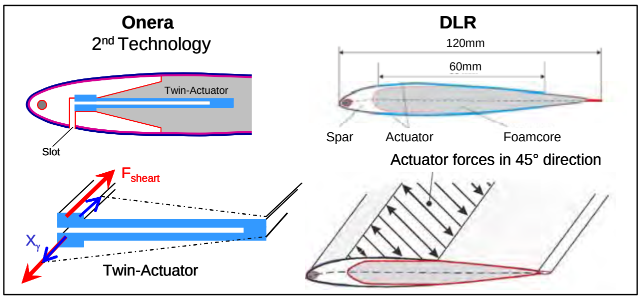

Figure 37: Sketch of active twist working principles at Onera and DLR.

A direct comparison of the 2nd generation TWISCA and the second generation DLR blade (AT2) is given in [77]. One blade of each concept has been tested on DLR's model whirl test rig. Both blades use Bo 105 blade planforms, but articulated blade attachment. Both blades were Mach-scaled with a radius of 2m. During testing both blades experienced failures of actuators. While for the TWISCA concept there is presently no repair technique, there is one for the DLR concept. In case of a burn-out failure, the failure is milled out and the hole is filled with epoxy resin. Such burns are usually small in size, and only a narrow stripe in the actuator becomes inactive. Figure 38 compares tip twist amplitudes for both blades. It can be seen that TWISCA generates higher amplitudes at lower forcing frequencies, AT2 at higher. Whereas AT2 shows a torsion frequency close to *4/rev*, TWISCA shows one at about *2/rev*. While the DLR blade was tested at 1043rpm, the Onera blade was tested up to 960rpm. The values in the figure correspond to 750rpm which was caused by a failure of one inner actuator at that speed that did not allow to do further testing.

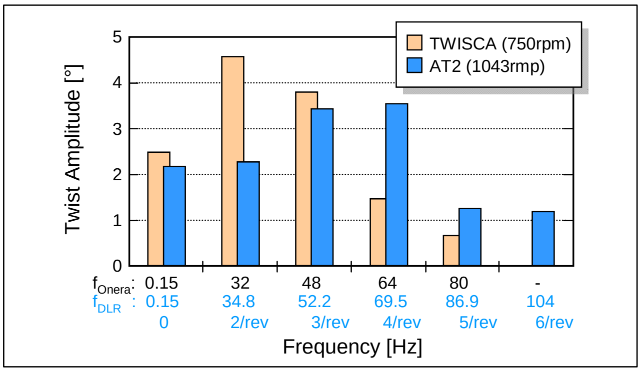

Figure 38: Tip Twist angles of TWISCA and AT2 blades.

Currently, DLR is manufacturing its 6th blade generation within the internal AcTOR project (Active Twist Optimised Rotor) using internal funding. The project aims to manufacture a 4-bladed rotor similar to Bo 105 (articulated hub instead of hingeless) and to perform functionality tests in DLR's rotor test hall prior to wind tunnel test. Wind tunnel tests in the DNW (German-Dutch Wind Tunnels) low-speed facility are planned under the international partnership of the STAR[7] (Smart Twisting Active Rotor) consortium. The STAR team presently prepares the necessary steps for such an international wind tunnel test campaign.

Ref. [78] outlines briefly two numerical models to describe the active twist. One is based on the active twist generated by an actuator element (TA), the other on the torsional moment (TM). Figure 39 compares the predicted blade tip pitch angles of both models to measurements using the AT3 blade. The AT3 blade uses again MFC patches that have been integrated into the lower und upper skin of the blade. Six individually controllable segments are applied to each side of the blade (the innermost segment consists of two MFC elements). Rotor radius was 2m and pre-twist -8°. The NACA 23012 airfoil was used up to 1.5m radius and the OA209 airfoil at the tip. The tip also showed a parabolic plan form. The left diagrams of Figure 39 show the tip pitch angles for different active segments, the photo on the right hand side (bottom) shows the AT3 blade installed on DLR's hover test stand and the diagram on the top right shows computed twist angle distributions of first and second twist mode for two different harmonic excitations.

[7] Contact: Dr. van der Wall, DLR, berend.vanderwall@dlr.de

Although the two numerical models differ from the measurement and hence need some improvement, a new idea of control actuation becomes evident and shall be outlined here. Instead of actuating each MFC segment in phase with the others, it might be beneficial to control segments individually. The figure top left shows a maximum of approx. 0.6° in measured tip pitch angle, if the three innermost segments are active and the three outermost are switched off (labelled as segments 1-3 in the figure). In contrast to that about 0.4° tip pitch was measured when all six segments were controlled simultaneously (labelled as segments 1-6 in the figure). This maximum can be further increased (bottom left) by controlling the two inner- and three outermost segments in counter-phase (labelled as $(1\text{-}2)^+$ & $(4\text{-}6)^-$) while a minimum was measured when the same elements were controlled in phase (labelled as $(1\text{-}2)^+$ & $(4\text{-}6)^+$). This can be explained by the excitation of the second torsion mode by the *6/rev* control (top right). The second mode's phase is changed by the counter-phase actuation of the outer segments such that both modes are working in phase and therefore add up at the blade tip. The effect is small, but tailoring the blade dynamics to the possibilities offered by active twist control in this respect might give much larger blade tip deflections than shown in the figure below.

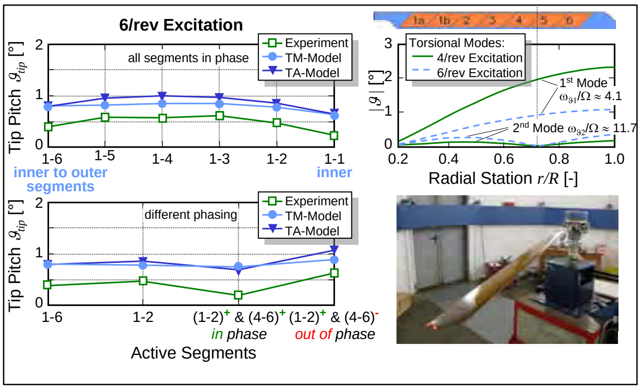

Figure 39: AT3 blade tip pitch angles for *6/rev* actuation.

A presentation on the technology and manufacturing process of active twist actuators is given in [79]. The utilization of multi-layer technology for low-profile piezo-composites may allow a reduction of the operation voltage, which is still much too high for rotorcraft applications.

Three issues need to be addressed for active twist. The first is the fatigue problem. Modern rotor blades have an effectively infinite life and have to be overhauled from time to time due to erosion etc. The question will be, if this is still the case for integrated actuation, since rotor blades work in a harsh environment (atmospheric temperature range, humidity, lightning strikes, centrifugals loads, elastic bending and torsion etc.). The second issue is the maintenance of the actuators itself. Eurocopter's flap system unit can be taken out of the blade for maintenance. Parallel to research on smart twist itself, repair methods need to be developed, e.g. to service short circuits. At least for the skin-integrated actuators there is a repair method [77]. The third issue is the measurement of the twist itself. It will be hardly possible to manufacture identical actuators/blades. Measuring the twist for an inner closed-loop control becomes important. The use of strain gauges might be problematic. This problem needs to be addressed in the future.

2.4. Multi-Swashplate Actuation

The advantage of HHC is its simplicity. However, IBC is superior in addressing several objectives at the same time. But, actuation systems in the rotating frame bear a technical risk and all concepts need to answer questions as costs, maintenance effort, durability etc. These considerations led to the idea of a multi-swashplate arrangement [80].

HAM describes the idea of IBC based on a conventional swashplate [17]. As long as the number of control degrees-of-freedom would equal the number of blades, IBC would be feasible. The multi-swashplate follows this idea. A single swashplate is sufficient for three or less rotor blades. For 4 to 6 blades, a second, concentric swashplate will be added. The first 2 or 3 blades are linked to the first swashplate, the remaining ones to the second. Such an IBC concept would cover most production helicopters worldwide. For more than 6 blades, a third swashplate will be required, but the system becomes rather complex in this case. The idea of multi-swashplate arrangements has not been investigated so far and comprises the advantages of HHC (no actuation in the rot ating frame) without its drawbacks. The rotor can be designed as usual without any modifications that result from actuator integration. The swashplate is a proven and reliable means to transfer control signals from the fixed to the rotating frame. The solution has low technical risk and might also be suitable as retrofit solution for existing helicopters. Figure 40 shows an example of a "true" IBC actuation.

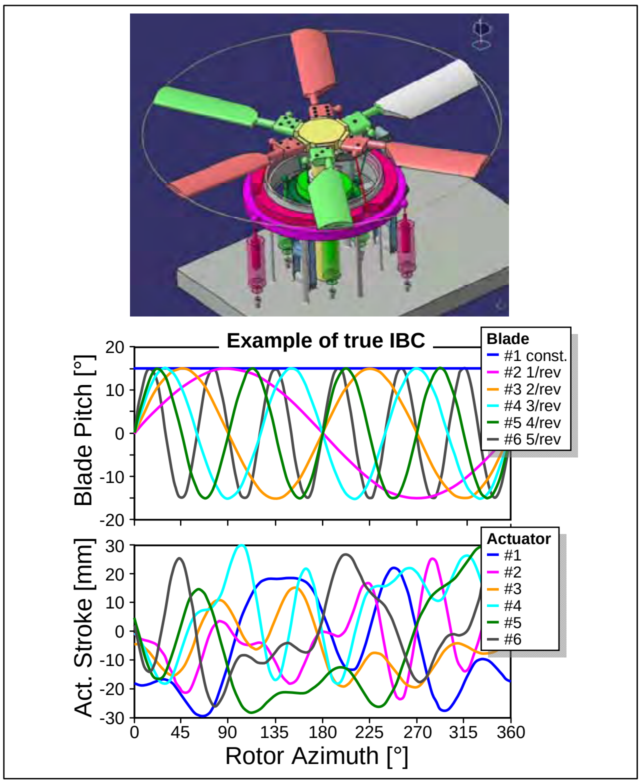

Figure 40: Example of "true" IBC for 6-bladed rotor.

For clarity: this example is just for demonstration purposes and does not reflect any reasonable IBC application. It depicts the ability to control arbitrary pitch histories with such a system. Pictured in the top is a 6-bladed rotor with two concentric swashplates. Each swashplate is linked to three blades and is actuated for simplicity by three boosters. Blade #1 has a constant pitch, blade #2 a *1/rev* variation, blade #3 a *2/rev* variation and so on. This is shown in the time history (middle). The bottom figure shows the corresponding booster strokes. The application of three boosters per swashplate is a drawback of this design, but other concepts overcome this problem and rely on three primary boosters as any other helicopter. Currently, a multi-swashplate arrangement for a 4-bladed rotor is being designed and manufactured for DLR's test rig. One design issue is to guarantee the same control stiffness and kinematic relations for both swashplates. Wind tunnel testing in the DNW is envisaged.

3. SWASHPLATELESS HELICOPTERS

At the early stage of helicopter development the swashplate reduced the control problem of the rotor blades tremendously. Since then, almost all helicopters featured a swashplate. An alternative is the control spider (e.g. Lynx). Swashplate or spider link the control law of one blade to that of the other blades. Each blade does the same, just phase-shifted. In addition, the swashplate and its various rods and levers generate parasite drag. This might be alleviated by fairings. In a consequent extension of this idea the Integrated Dynamic System (IDS) of the HAL Dhruv covers the whole control system by a rotor mast with large diameter. However, this generates new problems, e.g. precheck prior to flight and maintainability. Therefore, active rotor control was proposed to abandon the swashplate [18].

KRETZ [81] proposed the concept of a swashplateless helicopter. He stated that the swashplate introduces one of the most stringent limitations of the rotor by coupling the blades and imposing monocyclic pitch variation. The freedom of the blade to counteract an external disturbance does not exist. He presented a study based on the Alouette II rotor hub. The swashplate was replaced by a non-tilting plate. The outer rotating rim of this plate carried 3 electro-hydraulic actuators. The oil pump was integrated into the hub and was driven by the shaft to avoid hydraulic slip rings. Each actuator controlled the pitch of its blade independent of the others.

Preliminary design of an individual blade control system independent of a swashplate (IBIS) at Bell was presented in [82]. Design target was to place the individual actuators in the rotating system. Early designs tried to integrate the actuators into the rotor shaft, till heat problems emerged. This led to the concept of hub-integrated actuators. The final result of this design study was the IBIS concept shown in Figure 41. Each blade featured two pitch horns and four actuators per blade (2.8lb weight each) in a jam-tolerant configuration. Two hydraulic power supplies were above the hub and two below. They were driven by stationary gears that were attached to two standpipes. Basis helicopter for the design was a Bell 412. Each actuator was designed to generate 1270lb force and 2.75in stroke for a total blade pitch of 40° (16° collective, 24° cyclic). A parasite drag area reduction of 40% was determined (2.91ft² instead of 4.91ft²). Based on military requirements (ballistic protection etc.) a total IBIS weight of 335lb was predicted.

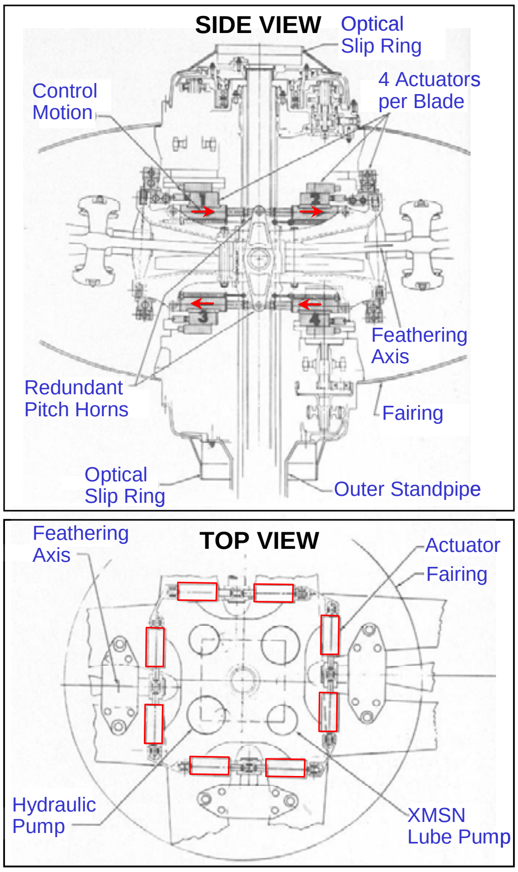

Figure 41: IBIS concept.

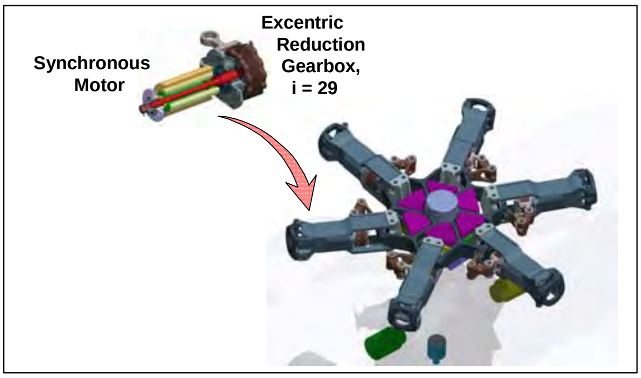

Figure 42: Swashplateless control for 19to helicopter.

A different way was followed in [83][8]. The target helicopter was similar to a CH-53G. The actuator requirements covered primary control and IBC. To alleviate the actuator power requirements at extreme manoeuvres in the corners of the flight envelope, IBC was intended to be phased out partly. The possibility to recover power from actuators that were driven by external pitching moments was considered. Different hydraulic actuation systems were considered, but brushless DC motors in combination with a reduction gearbox were finally chosen in a jam-free arrangement. The final variant is shown in Figure 42. The rotor featured a titanium hub with elastomeric blade flap-lag-pitch bearing. The actuator is placed inside a force carrying tube. A scissor unit counteracts the pitching moment. The overall weight was estimated to be 790kg and fell within 3% of the benchmark system including a retrofit IBC system. Reli-

[8] Partners were ZFL, Technical Universities Hamburg Harburg and Braunschweig, DLR

ability and safety aspects as well as the reconfiguration of degraded actuators were thoroughly investigated.

Flap control might be capable in the future of providing primary flight controls [53]. Therefore, active flaps are investigated for swashplateless rotor concepts. Some try to design new actuators that can provide sufficient deflections, others focus on the possibility to reduce amplitude requirements. Recently, two studies have been presented that use large stroke actuators driving a trailing edge flap [84], [85]. The first is an electro-mechanical actuator (EMA), the other a pneumatic artificial muscle (PMA). Both concepts address the application of IBC for vibration, noise etc., but also primary flight control. The EMA is integrated in a 4-bladed Sikorsky S-434 rotor. The application of this concept is expected to focus on larger rotors in Sikorsky's product line. Whirl testing was done in 2009. The EMA was tested from steady to *5/rev* actuation. The maximum flap deflection for *0/rev* and *1/rev* was ±10°. For the IBC application, special interest focuses on high amplitude *2/rev* control for performance improvement. The flap is a 24% chord and 12% span flap. It was centred at 72% radius. The geometric trailing edge flap rotation stops are ±15°, although all design conditions were within ±10°. The concept is shown in Figure 43. To amplify blade pitching by flap actuation the torsional frequency of the blade was altered by replacing the rotating pitch links by variable stiffness root springs. The whirl tower tests successfully demonstrated the ability of the EMA to operate in the 750g field of the test rotor. The actuators produced the expected torsional moments at all excitation frequencies. A second generation EMA was designed and fabricated. A wind tunnel test campaign is scheduled in 2010.

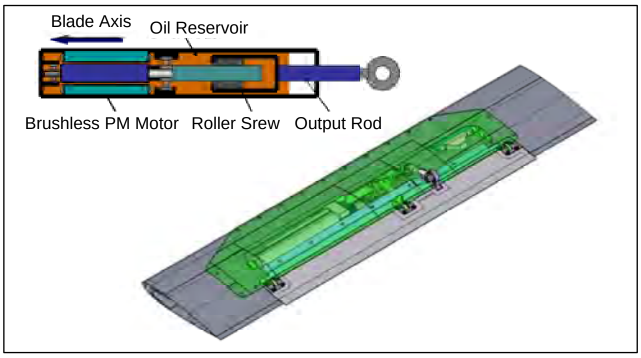

Figure 43: Schematic of EMA design elements and view of flap section from lower surface.

PMAs offer high energy densities at low weight and axial contractions of up to 25% of their length [85]. The trailing edge flap was sized for a Bell 407 rotor. The flaps are actuated by a pair of PMAs. Design goal was a flap deflection of ±7.5° to ±10° at frequencies up to *5/rev* (35Hz for the Bell 407). The second goal was to achieve even larger flap deflections at *1/rev* cyclic control to prove the actuator's primary control potential. Deflections of ±15° to ±20° were mentioned to be sufficient. The flap dimensions were 16% radial and 15% chordwise span with centre at 0.83R. A 27% scaled 1-bladed rotor model was built. Rotor speed of the scaled model was chosen to meet the centrifugal force (CF) of the Bell 407. The whirl test was conducted in a vacuum chamber. Aerodynamic forces were simulated by springs. Figure 44 shows the system design concept (right) and the effect of CF on flap deflection (left). Although the actuator performance degrades with CF loading, the initial goals have been met. Since the system was run at 60% of its maximum operating pressure it is believed that this margin could be used to compensate for this reduction.

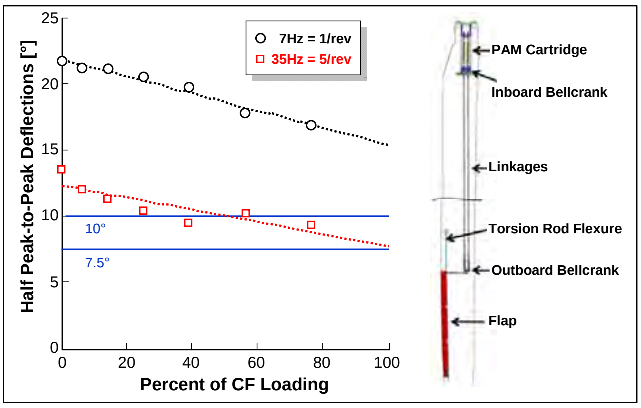

Figure 44: PMA system design concept (right) and effect of CF loading on flap deflection (left).

Other studies try to reduce cyclic pitch trailing edge flap deflection requirements by control of the horizontal tail [86]. However, the integration of the empennage into the overall control law increases system complexity and costs even further. The reduction of flap deflection requirements is addressed in [87], too. Pitch index as well as rpm variations were investigated for this purpose. The study also addresses aerodynamic power penalties of large trailing edge flaps. The study was based on a UH-60A like helicopter with torsional frequency reduced to *2.1/rev*. The flap was 20% in chord and extended from 70% to 90% radius. The numerical model used rigid flap and torsion blade element theory and prescribed wake. Power requirements in comparison to the baseline UH-60A were computed. At advance ratios below 0.2 the power increased for the swashplateless design by 2-4%, depending on the pitch index, i.e. higher pitch index caused higher power required. At high advance ratios (μ = 0.3) power requirements were approx. 6.5 to 7.5% higher at reversed impact of pitch index. The trailing edge deflections and the increase in aerodynamic drag are the cause for this aerodynamic power requirement. However, omitting the swashplate reduces parasite drag and thus power required. The idea of a swashplateless helicopter requires either blade root actuators for each blade or a central actuator with an adequate leverage system for indexing. The increase in system complexity will be significant. Finally, increasing rpm revealed a reduction in maximum flap deflections on the cost of increased rotor power required. Increasing rpm will also raise rotor noise. This does not seem to be practical.

Eurocopter, ZFL and DLR are investigating flap supported swashplateless rotor control concepts, too, see Figure 45. However, in contrast to the previous studies, the blade root actuators do not only provide simple indexing, but also some cyclic control. The flap provides manoeuvre margin and alleviates the requirements for the blade root actuator compared to [83]. IBC and high bandwidth collective control could be further flap applications. Finally, both actuators could be used for reconfiguration purposes.

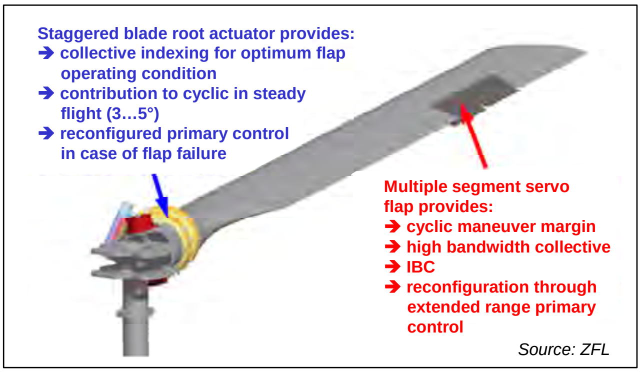

Figure 45: Swashplateless rotor control concept.

A rotor-based control system must be safe, durable, reliable, easy to maintain and have minimum weight and drag [82]. A swashplate is a proven and reliable system and it is cheap. Swashplateless concepts must compete with this and each benefit is of a more academic nature, if safety cannot be guaranteed. It might be therefore not helpful, if more and more control surfaces are integrated into the overall control scheme. And such a system must be of comparable weight as a conventional system including classical controls, passive absorbers and maybe IBC.

4. CONCLUSIONS

The challenges of helicopter deficiencies such as noise, vibrations, power required etc. have been discussed. One way out is active rotor control. Active rotor control can be implemented as HHC or IBC. IBC can be realised by a number of different concepts, ranging from HHC-like multi-swashplate solutions with actuators in the fixed frame to concepts using distributed smart actuators for active twist. The benefits of HHC and IBC have been proven many times. IBC turned out to be superior to HHC due to fewer constraints. IBC can alleviate a lot of typical helicopter problems:

- halve the BVI and in-plane radiated noise,
- reduce the cabin vibration by 80% or even more,
- reduce component loads and power required,
- alleviate blade stall,
- improve in-flight tracking,
- improve flap stability at high advance ratios

and so on. That is the good news. And now the bad: About 58 years of research and development on HHC and IBC have passed by. And no helicopter is equipped with such a system. More years will even pass by. Surely, this is attributed to the challenging requirements in which the helicopter and especially its rotor have to work, but also to little focused research (too many concepts), little harmonized work (duplication of results at various companies or institutions instead of cooperation; the HART projects are a good example of joint research and testing), more evolutionary trial and error work than straightforward engineering. Most critical however might be a certain lack of willingness to really push IBC to maturity for an application in helicopters. But even for customers it might be difficult to see an advantage of IBC and a payback. Manufacturers and operators have to earn money with their helicopters. An IBC system would surely raise the purchase price. And there has to be a reimbursement of these additional costs. On the other side, designs get more and more complex, the swashplateless concepts are the far end of this complexity. It should be questioned if this is still reasonable. The advice would be, make one step after the other, do not try to do two at the same time.

LITERATURE

AHS = American Helicopter Society
ARC = Aeronautical Research Council
ERF = European Rotorcraft Forum

[1] Kessler, C.: *Active Rotor Control for Helicopters: Motivation and Survey on Higher Harmonic Control*, 36th ERF, Paris, France, September 7-9, 2010.

[2] Friedmann, P.P., Millot, T.A.: *Vibration Reduction in Rotorcraft Using Active Control: A Comparison of Various Approaches*, Journal of Guidance, Control, and Dynamics, Vol. 18, No. 4, pp. 664 – 673, July-August, 1995.

[3] Chopra, I.: *Status of Application of Smart Structure Technology to Rotorcraft Systems*, Journal of the AHS, Vol. 45, No. 3, pp. 228 - 252, 2000.

[4] Padthe, A.K., Liu, L., Friedmann, P.P.: *A Comprehensive Study of Active Microflaps for Vibration Reduction in Rotorcraft*, 66th Annual Forum of the AHS, Phoenix, AZ, May 11-13, 2010.

[5] Leon, O., Hayden, E., Gandhi, F.: *Rotorcraft Operating Envelope Expansion Using Extendable Chord Sections*, 65th Annual Forum of the AHS, Grapevine, TX, May 27-29, 2009.

[6] Kobiki, N., Natsuki, K., Shigeru, S., Takeshi, A., Yasutada, T.: *Active Tab, a New Active Technique for Helicopter Noise Reduction*, 29th ERF, Friedrichshafen, Germany, September 16-18, 2003.

[7] Kobiki, N., Saito, S., Kosaka, M., Fuse, H.: *A Study of Closed Loop Control of Active Tab with BVI Detection Method for Helicopter Noise Reduction*, 32nd ERF, Maastricht, The Netherlands, September 12-14, 2006.

[8] Young, L.A.: *Systems Engineering: When Knowledge and Technology are the Product*, 64th Annual Forum of the AHS, Montreal, Canada, April 29-May 1, 2008.

[9] Matalanis, C.G., Kuczek, A., Lin, R.-S., Manes, E., Wake, B.E., Yeh, J., Chaudhry, Z., Brewer, P.: *Development of an Active Trim Tab System for Onboard Rotor Tracking*, 66th Annual Forum of the AHS, Phoenix, AZ, May 11-13, 2010.

[10] Martin, P.B., McAlister, K.W., Chandrasekhara, M.S., Geissler, W.: *Dynamic Stall Measurements and Computations for a VR-12 Airfoil with a Droop Leading Edge*, 59th Annual Forum of the AHS, Phoenix, AZ, May 6-8, 2003.

[11] Geissler, W., Dietz, G., Mai, H., Junker, B.: *Dynamic Stall Control Investigation on a Full Size Chord Blade Section*, 30th ERF, Marseille, France, September 14-16, 2004.

[12] Maucher, C.K., Grohmann, B.A., Jaenker, P., Altmikus, A., Jensen, F., Baier, H.: *Actuator Design for the Active Trailing Edge of a Helicopter Rotor Blade*, 33rd ERF, Kazan, Russia, September 11-13, 2007.

[13] Bernhard, A.P.F., Chopra, I.: *Mach-Scale Design of a Rotor-Model with Active Blade Tips*, 55th Annual Forum of the AHS, Montral, Canada, May 25-27, 1999.

[14] Bernhard, A.P.F., Chopra, I.: *Hover Test of a Mach-Scale Rotor Model with Active Blade Tips*, Journal of the AHS, Vol. 47, No. 4, pp. 273 - 284, 2002.

[15] Ham, N.D.: *Helicopter Individual-Blade-Control Research at MIT 1977-1985*, Vertica, Vol. 11, No. 1/2, pp. 109 - 122, 1987.

[16] Ham, N.D.: *Helicopter Individual-Blade-Control: Promising Technology for the Future Helicopter*, 21st ERF, Saint Petersburg, Russia, August 30-September 1, 1995.

[17] Ham, N.D.: *Helicopter Gust Alleviation, Attitude Stabilization, and Vibration Alleviation using Individual-Blade-Control Through Conventional Swash Plate*, 41st Annual Forum of the AHS, Fort Worth, Texas, May 15-17, 1985.

[18] Ham, N.D.: *A Simple System for Helicopter Individual-Blade-Control Using Modal Decomposition*, Vertica, Vol. 4, No. 1, pp. 23 - 28, 1980.

[19] Ham, N.D.: *A Simple System for Helicopter Individual-Blade-Control and its Application to Gust Alleviation*, 6th ERF, Bristol, England, September 16-19, 1980.

[20] Ham, N.D., Behal, B.L., McKillip R.M.: *Helicopter Rotor Lag Damping Augmentation through Individual-Blade-Control*, Vertica, Vol. 7, No. 4, pp. 361 - 371, 1983.

[21] Reichert, G., Arnold U.T.P.: *Active Control of Helicopter Ground and Air Resonance*, 16th ERF, Glasgow, Scotland, September 18-20, 1990.

[22] Kessler, C., Reichert, G.: *Active Control to Augment Rotor Lead-Lag Damping*, The Aeronautical Journal, Vol. 102, No. 1011, pp. 245 – 258, May, 1998.

[23] Quackenbush, T.R.: *Testing and Evaluation of a Stall-Flutter-Suppression System for Helicopter Rotors Using Individual-Blade-Control*, Journal of the AHS, Vol. 39, No. 2, 1984.

[24] Nguyen, K.: *Active Suppression of Stall on Helicopter Rotors*, 25th ERF, Rome, Italy, September 14-16, 1999.

[25] Richter, P., Blaas, A.: *Full Scale Wind Tunnel Investigation of an Individual Blade Control (IBC) System for the Bo105 Hingeless Rotor*, 19th ERF, Cernobbio, Italy, September 14-16, 1993.

[26] Jacklin, S.A., Swanson, S., Blaas, A., Richter, P., Teves, D., Niesl, G., Kube, R., Gmelin, B., Key, D.L.: *Investigation of a Helicopter Individual Blade Control (IBC) System in Two Full-Scale Wind Tunnel Tests*, Volumes I+II, NASA TP-2003-212276+7, 2003.

[27] Arnold, U.T.P., Mueller, M., Richter, P.: *Theoretical and Experimental Prediction of Individual Blade Control*, 23rd ERF, Dresden, Germany, September 16-18, 1997.

[28] Richter, P., Eisbrecher, H.-D.: *Design and First Flight Tests of Individual Blade Control Actuators*, 16th ERF, Glasgow, Scotland, September 18-20, 1990.

[29] Teves, D., Kloeppel, V., Richter, P.: *Development of Active Control Technology in the Rotating System, Flight Testing and Theoretical Investigations*, 18th ERF, Avignon, France, September 15-18, 1992.

[30] Schimke, D., Arnold, U.T.P., Kube, R.: *Individual Blade Control Demonstration Evaluation of Recent Flight Tests*, 54th Annual Forum of the AHS, Washington, DC, May 20-22, 1998.

[31] Morbitzer, D., Arnold, U.T.P., Mueller, M.: *Vibration and Noise Reduction through Individual Blade Control - Experimental and Theoretical Results*, 24th ERF, Marseille, France, September 15-17, 1998.

[32] Mueller, M., Arnold, U.T.P., Morbitzer, D.: *On the Importance and Efficiency of 2/rev IBC for Noise, Vibration and Pitch Link Load Reduction*, 25th ERF, Rome, Italy, September 14-16, 1999.

[33] Bebesel, M., Roth, D., Pongratz, R.: *Reduction of BVI Noise on Ground – Inflight Evaluation of Closed-Loop Controller*, 28th ERF, Bristol, UK, September 17-20, 2002.

[34] Roth, D.: *Advanced Vibration Reduction by IBC Technology*, 30th ERF, Marseille, France, September 14-16, 2004.

[35] Dieterich, O.: *Application of a Modern Control Technology for Advanced IBC Systems*, 24th ERF, Marseille, France, September 15-17, 1998.

[36] Kessler, C., Fuerst, D., Arnold, U.T.P.: *Open Loop Flight Test Results and Closed Loop Status of the IBC System on the CH-53G Helicopter*, 59th Annual Forum of the AHS, Phoenix, AZ, May 6-8, 2003.

[37] Fuerst, D., Kessler, Ch., Auspitzer, T., Mueller, M., Hausberg, A., Witte, H.: *Closed Loop IBC- System and Flight Test Results on the CH-53G Helicopter*, 60th Annual Forum of the AHS, Baltimore, MD, June 7-10, 2004.

[38] Fuerst, D., Arnold, U.T.P.: *Closed Loop IBC Results from CH-53G Flight Tests*, Aerospace Science and Technology, Vol. 9, No. 5, pp. 421 - 435, 2005.

[39] Norman, T.R., Shinoda, P.M., Kitaplioglu, C., Jacklin, S.A., Sheikman, A.: *Low-Speed Wind Tunnel Investigation of a Full Scale UH-60 Rotor System*, 58th Annual Forum of the AHS, Montreal, Canada, June 11-13, 2002.

[40] Jacklin, S.A., Haber, A., de Simone, G., Norman, T.R., Kitaplioglu, C., Shinoda, P.M.: *Full-Scale Wind Tunnel Test of an Individual Blade Control System for a UH-60 Helicopter*, 58th Annual Forum of the AHS, Montreal, Canada, June 11-13, 2002.

[41] Norman, T.R., Theodore C., Shinoda, P.M., Fuerst, D., Arnold, U.T.P., Makinen, S., Lorber, P., O´Neill, J.: *Full-Scale Wind Tunnel Test of a UH-60 Individual Blade Control System for Performance Improvement and Vibration, Loads, and Noise Control*, 65th Annual Forum of the AHS, Grapevine, TX, May 27-29, 2009.

[42] Friedmann, P.P.: *Vibration Reduction in Rotorcraft Using Actively Controlled Flaps – Their Evolution and Potential for Improving Rotorcraft Technology*, 30th ERF, Marseille, France, September 14-16, 2004.

[43] McCloud J.L., Evans, W.T., Biggers, J.C.: *Performance Characteristics of a Jet-Flap Rotor*, Conference on V/STOL and STOL Aircraft, NASA-SP 116, pp 29- 40, 1966.

[44] McCloud J.L., Kretz, M.: *Multicyclic Jet-Flap Control for Alleviation of Helicopter Blade Stresses and Fuselage Vibrations*, NASA-SP 352, pp 233- 238, 1974.

[45] Wei, F.-S., Weisbrich, A.L.: *Multicyclic Controllable Twist Rotor Data Analysis*, NASA-CR-152251, 1979.

[46] Millot, T.A., Friedmann, P.P.: *Vibration Reduction in Helicopter Rotors Using an Active Control Surface Located on the Blade*, 33rd AIAA/ASME/ASCE/AHS Structures, Structural Dynamics, and Materials Conference, AIAA-92-2451-CP, Dallas, TX, April 13-15, 1992.

[47] Cribbs, R., Friedmann, P.P.: *Actuator Saturation and its Influence on Vibration Reduction by Actively Controlled Flaps*, 42nd AIAA/ASME/ASCE/AHS Structures, Structural Dynamics, and Materials Conference, AIAA-2001-1467-CP, Seattle, WA, April 16-19, 2001.

[48] Depailler, G., Friedmann, P.P.: *Alleviation of Rotor Vibrations Induced by Dynamic Stall Using Actively Controlled Flaps with Freeplay*, 28th ERF, Bristol, UK, September 17-19, 2002.

[49] Patt, D., Liu, L., Friedmann, P.P.: *Rotorcraft Vibration Reduction and Noise Prediction Using a Unified Aeroelastic Response Simulation*, Journal of the AHS, Vol. 50, No. 1, pp. 95 - 106, 2005.

[50] Patt, D., Liu, L., Friedmann, P.P.: *Simultaneous Vibration and Noise Reduction in Rotorcraft Using Aeroelastic Simulation*, Journal of the AHS, Vol. 51, No. 2, pp. 127 - 140, 2006.

[51] Liu, L., Friedmann, P.P., Kim, I., Bernstein, D.S.: *Rotor Performance Enhancement and Vibration Reduction in Presence of Dynamic Stall Using Actively Controlled Flaps*, Journal of the AHS, Vol. 53, No. 4, pp. 338 - 350, 2008.

[52] Yeo, H.: *Assessment of Active Controls for Rotorcraft Enhancement*, Journal of the AHS, Vol. 53, No. 2, pp. 152 - 163, 2008.

[53] Fulton, M.V., Ormiston, R.A.: *Hover Testing of a Small-Scale Rotor with On-Blade Elevons*, Journal of the AHS, Vol. 46, No.2, pp. 96 - 106, 2001.

[54] Fulton, M.V., Ormiston, R.A.: *Small-Scale Rotor Experiments with On-Blade Elevons to Reduce Blade Vibratory Loads in Forward Flight*, 54th Annual Forum of the AHS, Washington, DC, May 20-22, 1998.

[55] Ormiston, R.A., Fulton, M.V.: *Aeroelastic and Dynamic Rotor Response with On-Blade Elevon Control*, 24th ERF, Marseille, France, September 15-17, 1998.

[56] Bernhard, A.P.F., Chopra, I.: *Trailing Edge Flap Activated by a Piezo-Induced Bending-Torsion Coupled Beam*, Journal of the AHS, Vol. 44, No.1, pp. 3 - 15, 1999.

[57] Roget, B., Chopra, I.: *Individual Blade Control for a Rotor with Dissimilar Blades*, Journal of the AHS, Vol. 48, No. 3, pp. 176 - 185, 2003.

[58] Roget, B., Chopra, I.: *Closed-Loop Test of a Rotor with Individually Controlled Trailing-Edge Flaps for Vibration Reduction*, Journal of the AHS, Vol. 55, No. 1, pp. 012009-1 - 012009-12, 2010.

[59] Kobiki, N., Tsuchihashi, A., Murashige, A., Yamakawa, E.: *Elementary Study for the Effect of HHC and Active Flap on Blade Vortex Interaction*, 23rd ERF, Dresden, Germany, September 16-18, 1997.

[60] Hasegawa, Y., Katayama, N., Kobiki, N., Nakasato, E.: *Experimental and Analytical Results of Whirl Test of ATIC Full Scale Rotor System*, 57th Annual Forum of the AHS, Washington, DC, May 9-11, 2001.

[61] Kobiki, N., Shigeru, S., Fukami, T., Komura, T.: *Design and Performance Evaluation of Full Scale On-Board Active Flap System*, 63rd Annual Forum of the AHS, Viginia Beach, VA, May 1-3, 2007.

[62] Kobiki, N., Shigeru, S.: *Performance Evaluation of Full Scale On-board Active Flap System in Transonic Wind Tunnel*, 64th Annual Forum of the AHS, Montreal, Canada, May 1-3, 2008.

[63] Crozier, P., Leconte, P., Delrieux, Y., Gimonet, B., Le Pape, A., des Rochettes, H.M.: *Wind-Tunnel Tests of a Helicopter Rotor with Active Flaps*, 32nd ERF, Maastricht, The Netherlands, September 12-14, 2006.

[64] Dieterich, O., Enenkl, B., Roth, D.: *Trailing Edge Flaps for Active Rotor Control: Aeroelastic Characteristics of the ADASYS Rotor System*, 62nd Annual Forum of the AHS, Phoenix, AZ, May 9-11, 2006

[65] Roth, D., Enenkl, B., Dieterich, O.: *Active Rotor Control by Flaps for Vibration Reduction - Full Scale Demonstrator and First Flight Test Results*, 32nd ERF, Maastricht, The Netherlands, September 12-14, 2006.

[66] Straub, F.K., Anand, V.R., Birchette, T.S., Lau, B.H.: *Wind Tunnel Test of the SMART Active Flap Rotor*, 65th Annual Forum of the AHS, Grapevine, TX, May 27-29, 2009.

[67] JanakiRam, R.D., Sim, B.W., Kitaplioglu, C., Straub, F.K.: *Blade-Vortex Interaction Noise Characteristics of a Full-Scale Active Flap Rotor*, 65th Annual Forum of the AHS, Grapevine, TX, May 27-29, 2009

[68] Sim, B.W., JanakiRam, R.D., Barbely, N.L., Solis, E.: *Reduced In-plane, Low Frequency Noise of an Active Flap Rotor*, 65th Annual Forum of the AHS, Grapevine, TX, May 27-29, 2009.

[69] Chopra, I.: *Development of a Smart Rotor*, 19th ERF, Cernobbio, Italy, September 14-16, 1993.

[70] Derham, R., Weems, D., Mathew, M.B., Bussom, R.: *The Design Evolution of an Active Materials Rotor*, 57th Annual Forum of the AHS, Washington, DC, May 9-11, 2001.

[71] Weems, D.B., Anderson, D.M., Mathew, M.B., Bussom, R.C.: *A Large-Scale Active Twist Rotor*, 66th Annual Forum of the AHS, Baltimore, MD, June 7-10, 2004.

[72] Wilbur, M.L., Mirick, P.H., Yaeger Jr., W.T., Langston, C.W., Cesnik, C.E.S., Shin, S.: *Vibration Reduction Testing of the NASA/ARMY/MIT Active Twist Rotor*, 57th Annual Forum of the AHS, Washington, DC, May 9-11, 2001.

[73] Shin, S., Cesnik, C.E.S., Hall, S.R.: *Closed-Loop Control Test of the NASA/ARMY/MIT Active Twist Rotor for Vibration Reduction*, 59th Annual Forum of the AHS, Phoenix, AZ, May 6-8, 2003.

[74] Monner, H.P., Opitz, S., Riemenschneider, J., Wierach, P.: *Evolution of Active Twist Rotor Design at DLR*, AIAA/ASME/AHS Adaptive Structures Conference, Schaumburg, IL, April 7 – 10, 2008.

[75] Opitz, S., Riemenschneider, J., Monner, H.P.: *Modal Investigation of an Active Twist Helicopter Rotor Blade*, 20th International Conference on Adaptive Structures and Technologies, Hong Kong, China, October 20-22, 2009.

[76] des Rochettes, H.M., Joly, D., Buchaniek, L., Leconte P.: *A New Concept of Active Twist Blade Applied to Main Rotor of Helicopter*, RTO Applied Vehicle Technology Panel Symposium, Evora, Portugal, RTO-MP-AVT-168, April 20-24, 2009.

[77] Riemenschneider, J., Opitz, S., Wierach, P., des Rochettes, H.M., Buchaniek, L.: *Structural Design and Testing of Active Twist Blades – A Comparison*, 35th ERF, Hamburg, Germany, September 22-24, 2009.

[78] Hoffmann, F., Opitz, S., Riemenschneider, J.: *Validation of Active Twist Modeling on Whirl Tower Tests*, 65th Annual Forum of the AHS, Grapevine, TX, May 27-29, 2009.

[79] Wierach, P.: *Low Profile Piezo Actuators Based on Multilayer Technology*, 17th International Conference on Adaptive Structures and Technologies, Taipei, Taiwan, October 16-19, 2006.

[80] Bartels, R., Kuefmann, P., Kessler, C.: *Novel Concept for Realising Individual Blade Control (IBC) for Helicopters*, 36th ERF, Paris, France, September 7-9, 2010.

[81] Kretz, M.: *Research in Multicyclic and Active Control of Rotary Wings*, Vertica, Vo. 1, No. 2 pp. 95 – 105, 1976.

[82] Guinn, K. F.: *Individual Blade Control Independent of a Swashplate*, Journal of the AHS, Vol. 27, No. 3, pp. 25 - 31, 1982.

[83] Arnold, U.T.P., Fuerst, D., Neuheuser, T., Bartels, R.: *Development of an Integrated Electrical Swashplateless Primary and Individual Blade Control System*, 32nd ERF, Maastricht, The Netherlands, September 12-14, 2006.

[84] Lorber, P.F., O'Neil, J.J., Isabella, B., Andrews, J., Wong, J., Hein, B., Geiger, D., Wake, B.E., Jonsson, U., Sun, F.: *Whirl Test of a Large Scale High Authority Active Flap Rotor*, 66th Annual Forum of the AHS, Phoenix, AZ, May 11-13, 2010.

[85] Woods, B.K.S., Kothera, C.S., Wereley, N.M.: *Whirl Testing of a Pneumatic Artificial Muscle Actuation System for a Full-Scale Active Rotor*, 66th Annual Forum of the AHS, Phoenix, AZ, May 11-13, 2010.

[86] Ghandi, F., Sekula, M.: *Helicopter Horizontal Tail Incidence Control to Reduce Rotor Cyclic Pitch and Blade Flapping*, 66th Annual Forum of the AHS, Baltimore, MD, June 7-10, 004.

[87] Duling, C., Ghandi, F., Straub, F.: *On Power and Actuation Requirement in Swashplateless Primary Control Using Trailing-Edge Flaps*, 66th Annual Forum of the AHS, Phoenix, AZ, May 11-13, 2010.